# The Synthesis and Evaluation of Thermally Stable Eu-doped Silicate Phosphors in White LEDs Application

# 白色LED応用における熱安定性を持つEu添加シリケート系蛍光体の合成および評価

A dissertation submitted in partial fulfillment of the requirements for the

Doctor of Engineering

by

**Siti Sarina Binti Nasir**

Academic Supervisor

**Associate Professor Ariyuki Kato**

Department of Information Science and Control Engineering

Nagaoka University of Technology

Nagaoka, Niigata, Japan

July 2021

# Abstract

The combination of blue LED and yellow phosphors are the simplest combination in the fabrication of white LEDs. It observed that yellow phosphors with high thermal stability are required to produce high-power- efficiency-white LEDs as it begins to deteriorate at 150 °C during operation. Generally, the most widely used blue excited yellow phosphors for white LEDs is YAG:$Ce^{3+}$ because of its high luminous efficiency and high chemical stability. However, there is a main problem regarding low thermal stability, which effect the power efficiency of white LEDs. To resolve this problem, silicate phosphors were investigated, which have high luminescent properties, physical, chemical stability and high thermal stability for the possibility replacement of YAG:$Ce^{3+}$ phosphors.

For the silicate phosphors, Eu is used as doping agent instead of Ce, which has high luminescent efficiency and the ionic radius of both Sr and Eu ions are almost same. Moreover, emission wavelength also can be tunable by modifying host lattice. Instead of using Garnet in YAG:$Ce^{3+}$ phosphor, alkaline earth orthosilicate phosphor were used. Besides that, Si sources can be easily found and existed in large quantities in the earth's crust according to Clarke number, indicating that silicate compound can get easily to synthesize the strontium silicate phosphors. In this study, Eu doped silicate phosphor were synthesized by improved polymerized complex method (PCM) using TEOS, which has advantages in the aspect of uniformity of atomic component of the samples and can be synthesized at low temperature.

The simplest compounds made from alkaline earth Sr, Si and O is $Sr_2SiO_4$. Therefore, $Sr_2SiO_4:Eu^{2+}$ phosphors were synthesized by improved PCM using TEOS as basic phosphors. Generally, $Sr_2SiO_4$ have two different crystal phases: (1) α' phase – high temperature phase and (2) β phase – low temperature phase, with phase transition at 85 °C. In this study, β phase $Sr_2SiO_4:Eu^{2+}$ phosphors were successfully synthesized by PCM using HCl under $H_2/N_2$ atmosphere at 1150 °C with 3% Eu concentration. The α'→β → α'phase transition and hysteresis of the samples can be observed. The appearance of proper phase transition indicates that β phase $Sr_2SiO_4:Eu^{2+}$ phosphors show good characteristics and properties by using improved PCM.

As $Sr_2SiO_4:Eu^{2+}$ phosphors have phase transition, Li was introduced to lock the phase transition in the host lattice. $Li_2SrSiO_4:Eu^{2+}$ silicate phosphor is one of the well-known yellow phosphors with high luminescent properties and was synthesized by improved PCM. The optimum synthesis of $Li_2SrSiO_4:Eu^{2+}$ phosphors are 900 °C under $H_2/N_2$ atmosphere and 0.5% Eu concentration. Eu concentration and temperature quenching of the samples were discussed. The PL intensity at 150 °C was about 80% compared to room temperature and obtained high activation energy (0.43 eV), indicating that $Li_2SrSiO_4:Eu^{2+}$ phosphors have high thermal stability compared to YAG:$Ce^{3+}$. The study show that $Li_2SrSiO_4:Eu^{2+}$ phosphors have high thermal stability and possibly applicable in high-power-efficiency white LEDs cation

# INDEX

# List of Figures

# List of Tables

# Chapter 1

# Introduction

## 1.1 General aspect

Before the modernization of technology, sun becomes the main source of light providing the sunlight and nutrients to humans, animals, and plants. During day night, the people ignited fire or flame by burning the woods and other burnable things as source of light to make their life easier. In 19th century, Thomas Edison who was the well-known American inventor had brought big changes in lightening field by inventing his own electric light bulb which is called Edison light bulb and widely gave impact on modern industrialized world [1.1]. From this turning point, there were many research regarding in lighting field until the invention of incandescence and fluorescent lamps were introduced, which were prevalent tools in lighting application for household, industrial and business. The common uses of fluorescent lamps are used in both indoors and outdoors decorative lightening, background for LCD display and others. However, these fluorescent lamps have several problems as small mercury were used in the tubes which dangerous to human health and flickers of the high frequency can be irritating to humans such as eye strain, headaches and migraines. For example, Minamata disease is known as neurological disease caused by severe mercury and it was huge outbreak epidemic in Japan [1.2–1.4]. The release of mercury in the industrial water waste from a chemical factory were naturally accumulated in the fish and shellfish. When the local people consume the effected fish or shellfish in daily life resulted in mercury poisoning. Due to this incident, Japan will prohibit the usage of mercury. Meanwhile, in Malaysia, the consumption of mercury in cosmetics and beauty care products, which were unregistered and uncertified by Minister Health of Malaysia by becomes huge issues as the price of those unregistered product

much cheaper than other established and registered products [1.5,1.6]. This problem gives high risk to the consumers' health and Minister Health of Malaysia takes strict measures to prevent the sales and manufacturing of any products containing these harmful substances. From mercury incidents in both countries, the usage of mercury brings more harm to the humans and nature.

To overcome the mercury problem in fluorescent lamps, over the years, recent development and commercialization of light emitting diodes (LEDs) are sought as feasible replacement for the aforementioned conventional lamps due to superior advantages in the aspects of energy consumption, thermal and chemical stability, long lasting, compactness and environmentally sustainable [1.7–1.9]. LEDs are the greatest invention in lightening fields by using phosphors because of the major energy saving, especially white LEDs are widely and practically used in our daily life nowadays. The research continues and never ending until now as the researchers make improvisation on white LEDs. Although LEDs are the greatest invention for now, there are also problems regarding thermal stability, sustainability, high power and others.

## 1.2 White LEDs

### 1.2.1 Combination of LEDs and phosphors

There are 3 basic combinations of LEDs and phosphors used in the fabrication of white LEDs as shown in Fig.1.1 [1.10–1.13].

(1) UV LED + (Red + Green + Blue) phosphors

(2) Blue LED + (Red + Green) phosphors

(3) Blue LED + yellow-orange phosphors

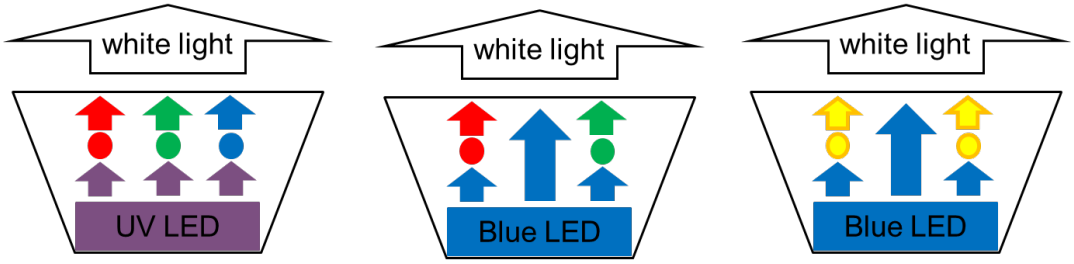


Fig.1.1 The combinations of white LEDs

The fabrication of white LEDs by using combination (1) and (2) requires high cost and the fabrication seems quite complicated. In other hand, most commercially available white LEDs use blue LED and yellow phosphors (combination (3)) such as InGaN blue LED $\lambda_{em}$ = 470 nm and $Y_3Al_5O_{12}:Ce^{3+}$ ($YAG:Ce^{3+}$) phosphor as a yellow phosphors [1.11–1.17]. The combination of blue LED and yellow phosphors are commonly used because of advantage in the simplicity for fabrication and low cost compared to other combinations. Although the combination (3) has problem regarding color rendering index, white LEDs can be fabricated with only a single phosphor and the optical properties of white LEDs can be easily adjusted, leading to the high conversion efficiency of the white LEDs. Besides that, compared with color conversion from UV light, the Stokes shift is small and the essential energy conversion can be improved. Lastly, the luminous efficiency is high because the transmitted light of blue LED can be used. White

LEDs that use these complementary colors is pseudo-white light, which humans recognize as a white color as the combination of yellow and blue light are located between green and red colors.

### 1.2.2 High-Power-Needed-Industry and Problem in Thermal Stability

Fishery industry are one of the big industries contributes economy in Malaysia and Japan, as both countries are surrounded by the sea. Before the modernization in lightening field, burning a fire on the seashore was basic technique to attract fish. Over the centuries, it has evolved into more technologically advanced by using high power white LEDs. High power white LEDs now plays a major role in commercial fishing especially squid fishing, contributing significantly to total catch yield and the profitability of many industrialized fisheries. Fig. 1.2 shows the spot of squid fishing light floating in the sea of Japan (night view as seen from the satellite) [1.18].

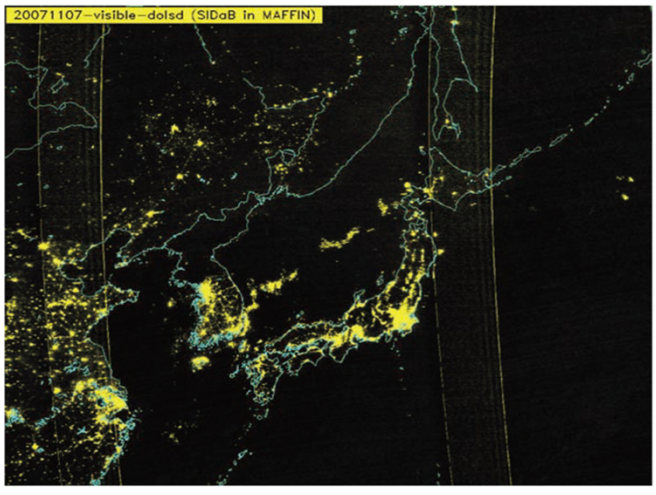


（出典：水産研究・教育機構 FRANEWS vol.18）

Fig. 1.2 The spot squid fishing light in Japan (night view) captured by the satellite [1.18]

Nowadays, high power white LEDs are required in heavy industry to small industry. Other than squid fishing, high power white LEDs are need in football stadium for possible long matches, food stalls business for more longer business duration at the night and others.

Generally, there are many aspects and characteristics are required to fabricate ideal white LEDs. The emission of white LEDs must be visible light or near UV light, which has suitable excitation spectrum for LED emission. High luminous and power efficiency, high thermal stability (produces well emission even at high temperature), stability of crystals at high temperatures (resistance to heat generation from LED), and chemical stability especially high durability against humidity are the crucial characteristics for the fabrication of ideal white LEDs. The temperature of operating white LEDs can be achieved at 100 °C above where the white LEDs can reduce in performance after 150 °C [1.19,1.20], which problem with yellow phosphor. To encounter to this problem, the materials or phosphors with high thermal (low temperature quenching) and chemical stability are required. As we all know, the most widely used blue excited yellow phosphors for white LEDs is YAG:$Ce^{3+}$ phosphors because of its high luminous efficiency and high chemical stability. However, there is problem regarding low thermal stability [1.13,1.15,1.17,1.21]. In order to solve this problem, new silicate phosphors with high thermal and chemical stability are synthesized in this study for the white LEDs application, which is possible replacement for YAG:$Ce^{3+}$ phosphors.

In this study, $Li_2SrSiO_4:Eu^{2+}$ yellow silicate phosphors were synthesized and the properties of the above silicate phosphors were in investigated. Both YAG:$Ce^{3+}$ and $Li_2SrSiO_4:Eu^{2+}$ are yellow phosphors with high in chemical and physical stability. According to previous report, $Li_2SrSiO_4:Eu^{2+}$ phosphors have higher luminous efficiency and thermal stability compared to YAG:$Ce^{3+}$ phosphors [1.22–1.27]. However, the thermal stability of $Li_2SrSiO_4:Eu^{2+}$ phosphors were not detailed investigated in the researches [1.23,1.28] and we

expect that $Li_2SrSiO_4:Eu^{2+}$ phosphors have higher thermal stability than $YAG:Ce^{3+}$ phosphors. Table 1.1 shows the comparison of the elements in $YAG:Ce^{3+}$ and silicate phosphors.

Table 1.1 Comparison of $YAG:Ce^{3+}$ and silicate phosphors

| $YAG:Ce^{3+}$ | $Sr_2SiO_4:Eu^{2+}$ & $Li_2SrSiO_4:Eu^{2+}$ |
|---|---|
| Y (Rare earth element) | Sr (Alkaline-earth metal) |
| Al (Post transition metal) | Si (Metalloids) |
| Ce (Rare earth) | Eu (Rare earth) |
| - | Li (alkaline metal) |

From the above table, Sr and Si exist in large quantities in the earth's crust compared to Y and Al. The abundance of the elements in the earth's crust will discussed briefly in section 1.3.1. In this study, Eu are used as doping agent as it has high emission efficiency and the emission wavelength can be easily adjustable or tuneable compare to Ce. The mechanism of Eu emission will be discussed briefly in the section 1.4.

## 1.3 Silicate phosphor

### 1.3.1 General aspects

The research about silicate phosphors were firstly introduced by Barry in 1968, where the fluorescence of $Eu^{2+}$ doped alkaline earth orthosilicate phosphors were firstly reported [1.29]. Rare earth doped silicate phosphors are promising candidates for white LED because of their good photoluminescence properties and chemical-physical stabilities provided by the tetrahedral silicate $(SiO_4)^{4-}$ [1.30–1.36]. Eu doping is necessary as activator or doping agent in the making of silicate phosphors which the ionic radius of both Sr and Eu ions are very close. On top of that, there are many silicon (Si) sources for silicate compound can be easily found and presented in the earth crust. The relative abundance of the elements on the earth are called Clarke number [1.37]. Generally, most of the elements do not occur free in nature, which present in single element. Most of the elements exist in chemical combinations with other elements. Table 1.2 shows the abundance of the elements in earth' crust. From the Table 1.2, the silicon is the 2nd most abundance elements exist in earth's crust, indicating that silicate compound can get easily to synthesize silicate phosphors. Therefore, many rare earths doped silicate phosphors can be synthesized in this study.

Table.1.2 The abundance of elements in earth's crust [1.37]

| Rank | Atomic Number | Elements | Abundance [mg/kg] | Clarke Number [%] |
|---|---|---|---|---|
| 1 | 8 | Oxygen | $4.61 \times 10^5$ | 49.5 |
| 2 | 14 | Silicon | $2.82 \times 10^5$ | 25.75 |
| 3 | 13 | Aluminium | $8.23 \times 10^4$ | 7.51 |
| ⋮ | | | | |
| 15 | 38 | Strontium | $3.70 \times 10^2$ | 0.017 |
| ⋮ | | | | |
| 25 | 58 | Cerium | $6.65 \times 10^1$ | no data |
| ⋮ | | | | |
| 29 | 39 | Yttrium | $3.30 \times 10^1$ | no data |
| ⋮ | | | | |
| 32 | 3 | Lithium | $2.00 \times 10^1$ | no data |
| ⋮ | | | | |
| 52 | 63 | Europium | $2.00 \times 10^0$ | no data |

From the above elements, the simplest compounds made from alkaline earth, Si and O is $Sr_2SiO_4$. Therefore, in this study, $Sr_2SiO_4:Eu^{2+}$ silicate phosphors were synthesized as basic phosphors. These phosphors show green emission with unique phase transition. As there is phase transition occur in $Sr_2SiO_4:Eu^{2+}$ phosphors, which is not applicable in white LEDs, $Li_2SrSiO_4:Eu^{2+}$ silicate phosphors as yellow phosphors by Li introduction were synthesized to fix the phase transition. The optical and thermal stability properties of $Li_2SrSiO_4:Eu^{2+}$ yellow phosphors were investigated for high power efficiency white LED application.

### 1.3.2 $Sr_2SiO_4:Eu^{2+}$ phosphors

$Sr_2SiO_4:Eu^{2+}$ silicate phosphors indicate green emission and has good features with high efficiency in light conversion for blue light and near UV LEDs in white LEDs application [1.38–1.43]. $Sr_2SiO_4:Eu^{2+}$ phosphor has unique properties, which have two main crystallographic phases in $Sr_2SiO_4$ host lattice; (1) high temperature α'- phase which applicable in white LEDs application and (2) low temperature β - phase which is applicable in thermochromic. The phase transition temperature between β ↔ α' phases is at 85 °C [1.44]. The Fig. 1.3 shows the crystal structure of both α' and β phases $Sr_2SiO_4$ and their characteristics are shown in Table 1.3.

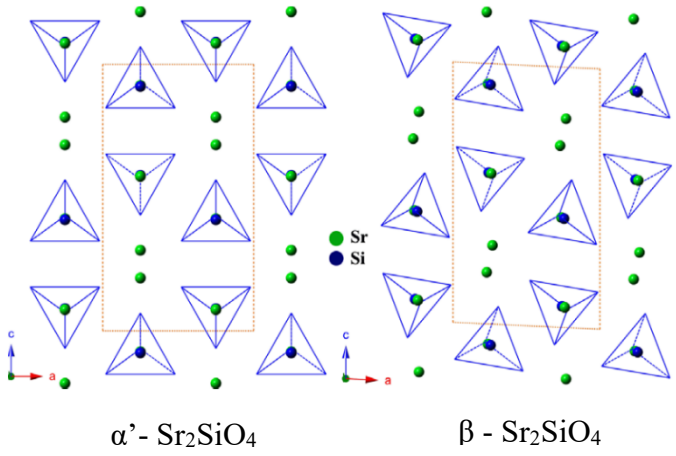


α'- $Sr_2SiO_4$ β - $Sr_2SiO_4$

Fig. 1.3 Crystal structure of $Sr_2SiO_4$ [1.45]

Table. 1.3 The characteristics of α' and β phases $Sr_2SiO_4$ [1.44,1.46]

| α'- $Sr_2SiO_4$ | β - $Sr_2SiO_4$ |
|---|---|
| high temperature (orthorhombic) | low temperature (monoclinic) |
| space group Pnmb | space group P21/n |
| a = 5.682 Å | a = 5.679 Å |
| b = 7.090 Å | b = 7.078 Å |
| c = 9.773 Å | c = 11.0395 Å |
| α = 90°, β = 90°, γ = 90° | α = 90°, β = 118.252°, γ = 90° |
| structure type $K_2[SiO_4]$ | structure type $Ca_2[SiO_4]$ |
| white LED application | thermochromic application |

On top of that, there are two cation sites corresponding to α' and β phases, Sr(1) and Sr(2), which have similar cooperative properties in both phases. Fig. 1.4 shows the coordinate chain of Sr(1) and Sr(2) sites. Sr(1) represents 10-coordinated sites from zigzag chains of Si-O-Sr(1)-O-Sr(2). Meanwhile, Sr(2) represents 9-coordinated sites form zigzag chain of (Sr(1)-O-Sr(2)-O-Sr(1)) along b-axis. The average Sr-O distance for Sr(1) sites is equal to 2.852 Å and 2.850 Å in both α' and β phases respectively. For Sr(2) sites, the average Sr-O distance is equal to 2.698 Å and 2.709 Å in both α' and β phases respectively. $Eu^{2+}$ ions substitute in $Sr^{2+}$ sites in the host lattice due to the similar ionic radius of $Eu^{2+}$ and $Sr^{2+}$ compared to the ionic radius of $Si^{4+}$ ions (Ionic radius of $Eu^{2+}$ is larger than $Si^{4+}$ ions) [1.47–1.49]. The substitution of $Eu^{2+}$ ions in both Sr(1) and Sr(2) sites, which have different crystal field, resulting the two broad bands in emission spectrum of $Sr_2SiO_4:Eu^{2+}$ phosphors; Eu(1) and Eu(2) emissions.

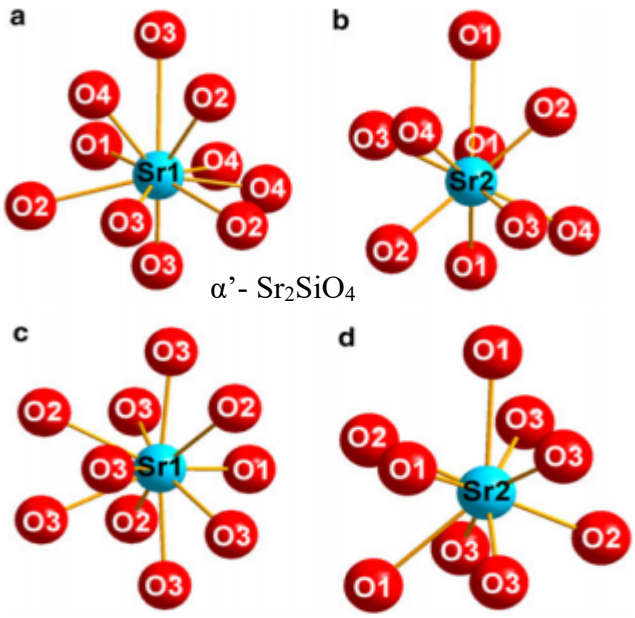


Fig. 1.4 Coordination chain of Sr(1) and Sr(2) sites [1.47]

Generally, it is difficult to obtain pure β phase at room temperature as α' phase samples are easily obtained at room temperature below 85 °C when impurities added. This phase transition leads to the change in emission of the samples and $Sr_2SiO_4:Eu^{2+}$ phosphors also attract attention as thermochromic materials [1.45]. L.C. Ju et al. also states that the samples can be turned to α' phase by doping small amount of Ba to stabilize the host lattice [1.47]. Eu doping is used for the synthesis of the phosphors in the application of white LEDs. Therefore, it is difficult to synthesis of β - $Sr_2SiO_4:Eu^{2+}$ phosphors due to the Eu doping acts as impurities and effect the crystallinity and phases of the phosphors. The effect of Eu doping including the limitation of Eu doping to obtain pure β - $Sr_2SiO_4:Eu^{2+}$ phosphors had not been fully investigated. Therefore, in this study, we successfully synthesized β - $Sr_2SiO_4:Eu^{2+}$ phosphors by improved polymerized complex method (PCM) using TEOS and the Eu doping limitation were investigated.

### 1.3.3 $Li_2SrSiO_4:Eu^{2+}$ phosphors

Among of silicate phosphors, $Li_2SrSiO_4:Eu^{2+}$ phosphors also attract attention owing to the advantages in the terms of high luminescent properties and physical-chemical stability. $Li_2SrSiO_4:Eu^{2+}$ phosphors shows yellow emission which is promising luminescent materials and possibly replaceable the conventional $YAG:Ce^{3+}$ yellow phosphors in white LEDs application. As $Sr_2SiO_4:Eu^{2+}$ phosphors have phase transition, it seems difficult to utilize the white LEDs application as the performances of white LEDs will be affected. Li introduction into to $Sr_2SiO_4:Eu^{2+}$ phosphors is to fix the phases in the host lattice. Table 1.4 show the characteristics of $Li_2SrSiO_4:Eu^{2+}$ phosphors.

Table. 1.4 Characteristics of $Li_2SrSiO_4:Eu^{2+}$ phosphors [1.50]

| | $Li_2SrSiO_4$ |
|---|---|
| structure | hexagonal crystal |
| space group | $P3_121$ |
| a [Å] | 0.50259 |
| b [Å] | 0.50259 |
| c [Å] | 1.2471 |

$Li_2SrSiO_4:Eu^{2+}$ phosphors are composed by three types of polyhedrons, which are $LiO_4$, $SrO_8$ and $SiO_4$ [1.51]. Two $LiO_4$ tetrahedra and one $SiO_4$ tetrahedron share O atom to form basic structural unit $[Li_2SiO_9]^{12-}$. This $[Li_2SiO_9]^{12-}$ and $SrO_8$ polyhedron share O atom to form the basic structural unit $[Li_2SrSiO_3]^{18-}$ (Fig. 1.5(a)). These basic structural units share O atom and form a parallel layer to (001) (Fig.1.5 (b)). These layers are stacked in the [001] direction for each unit cell to form a three-dimensional structure (Fig.1.5 (c)) [1.51]. Since $Sr^{2+}$ and $Eu^{2+}$ in the 8-coordinated structure have the same ionic radius ($Sr^{2+}$ = 1.26 Å, $Eu^{2+}$ = 1.25 Å), $Eu^{2+}$

ions substitute in $Sr^{2+}$ sites. $Sr^{2+}$ sites are completely substituted with $Eu^{2+}$ ions in $Li_2SrSiO_4:Eu^{2+}$ phosphors also have same crystal structure as shown in Fig. 1.6.

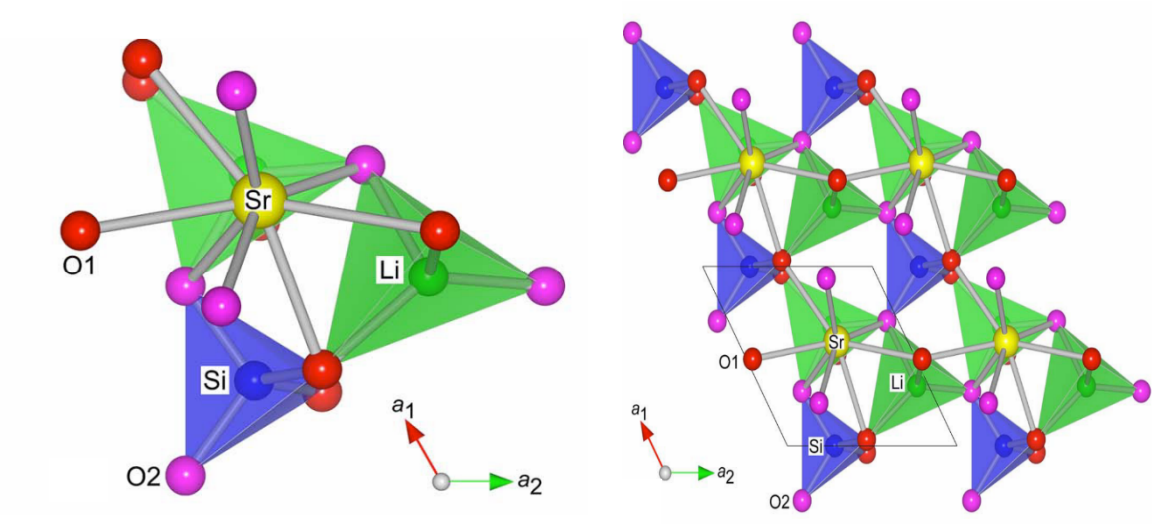


(a) $[Li_2SrSiO_3]^{18-}$ along c-axis

(b) 2D layers parallel to (001)

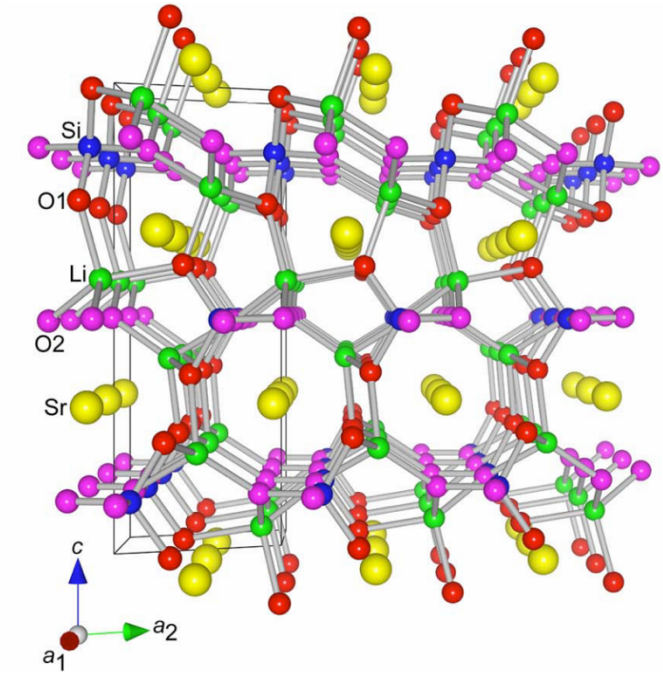


(c) the layers are stacked in the [001] direction to form 3D structure

Fig.1.5 Crystal structure of $Li_2SrSiO_4$ (undoped) [1.51]

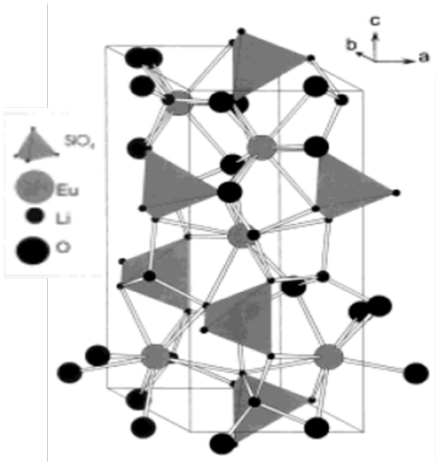


Fig. 1.6 Crystal structure of $Li_2SrSiO_4:Eu^{2+}$ phosphors [1.50]

## 1.4 Luminescent materials by Eu emission

### 1.4.1 The mechanism of emission

Generally, luminescent materials which are called phosphors mostly solid inorganic materials consists of host lattice and intentionally doping with small amount of emission ions (activators, luminescence center or doping agent). The mechanism of emission can be explained by configuration coordinate model in Fig.1.7 below. The configuration coordinate model is a potential curve that shows the energy when emission ions and the nearest ions are extracted and handled as independent molecules. The excitation light of the phosphors for white LEDs application is in low energy region such as blue light or near ultraviolet light. Therefore, light absorption and emission of emission ions occur in a relatively narrow range of emission ions and surrounding ions, which is good agreement with the configuration coordinate model.

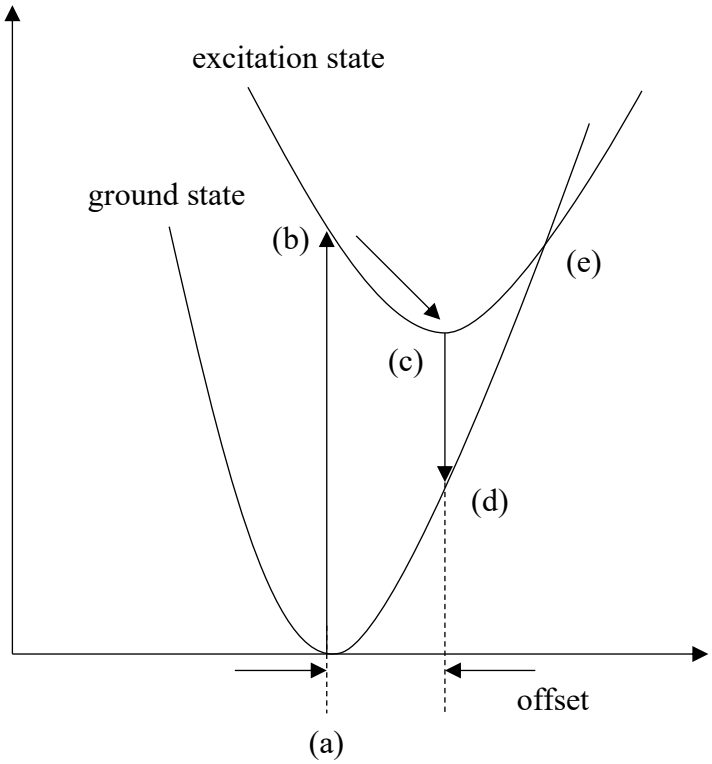


Fig. 1.7 Emission mechanism by configuration coordinate model

At first, emission ions absorbed the outer energy and the ions were excited from the ground state (a) to excitation state (b). The excited ions reach at the emission the emission level (c), which is one of the more stable excited states, while losing part of the energy due to heat. Lastly, the ions release light and return to the ground state (d). The most stable configuration of atoms in the excited state is different from that in the ground state. Since the excited state has higher energy than ground state, the electron orbits is getting bigger. As a result, the overlap of adjacent ions with the electron orbit increases and electrostatic repulsion also increases. In order to alleviate the electrostatic repulsion, the atoms move to a more stable equilibrium position while losing part of their energy due to thermal vibration. Since the nucleus is thousands to ten thousand times heavier than the electron mass, the ions are hardly to move during the transition from (a) to (b). This principle is called Frank-Condon principle [1.52].

The difference between the most stable configuration coordinates in the ground state and the excitation state is called offset. The energy difference between the absorbed light and the emitted light is called stokes shift.

### 1.4.2 Eu emission and energy level

Generally, Europium (Eu) which one of the rare-earth group elements acts as activators or doping agents, are commonly used in the synthesis of phosphors. This is because Eu has broad and wide emission which is easy to control the colors of the emission when doping in the host lattice. Eu have both divalent ions, $Eu^{2+}$ and trivalent ions, $Eu^{3+}$, where both ions have different wavelength, energy and emission bands. The transition of $Eu^{3+}$ ions are in 4f-4f transition, which show stable red emission. Meanwhile, in the case of $Eu^{2+}$ ions, the $Eu^{2+}$ ions are depending on the crystal structure of host lattice and has broad emission characteristic from UV to red emission due to 5f-4f transition. The Fig.1.8 show the transition of both $Eu^{2+}$ and $Eu^{3+}$ ions.

Therefore, phosphors materials doped with $Eu^{2+}$ ions have been studied extensively for lighting and display application due to their broad emission band and adjustable emission color. In order to obtain $Eu^{2+}$ ions, $Eu^{3+}$ ions in the host lattice, the samples must undergo reduction process. Conventionally, $Eu^{2+}$ ions can be obtained by reduction under $H_2$, $H_2/N_2$ or CO ambient. Fig.1.8 shows both $Eu^{2+}$ and $Eu^{3+}$ doped phosphors that synthesized in our study.

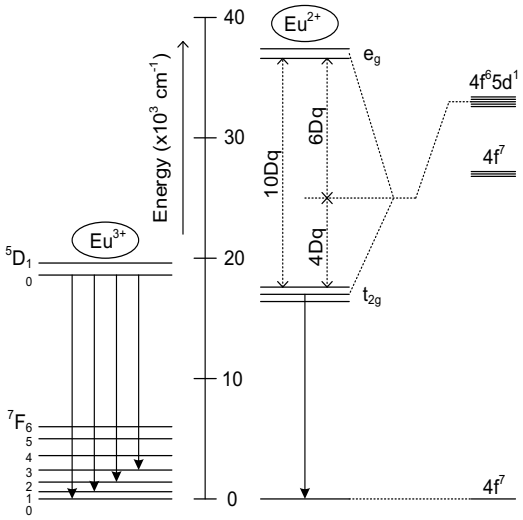


Fig.1.8 Mechanism of Eu emission

### 1.4.3 Configuration coordinate model and temperature quenching

Since the energy of the extended electron orbit is less sensitive to changes in coordination coordinates, the curve in the excited state becomes a parabola with a smaller curvature. Therefore, the excited state and the ground state intersect in (e) in Fig.1.7. White LEDs have a high temperature because phosphor mixed resin is mounted near the chip that generates heat. When used at such high temperatures, there is a high probability that energy will be lost beyond this intersection (e), and a phenomenon occurs in which the luminous efficiency decreases as the temperature rises. This phenomenon is called thermal quenching. To control thermal quenching, it is necessary to select a phosphor with the smallest possible offset.

## 1.5 Improved Polymerized Complex Method

Generally, solid-state reaction (SSR) is the most conventional method in synthesizing of the phosphors my mixing powder reactants and sintering to produce desired products [1.53]. There are many silicate phosphors also were synthesized by SSR method [1.41,1.47,1.54–1.56] as it is the easiest and simplest method. However, the disadvantages of SSR method are primarily on the inhomogeneity of the starting materials and difficult to control particle morphology. Besides that, high sintering temperature are required to synthesize the phosphors. Therefore, many synthesis methods were introduced such as hydrothermal processing, solvothermal, sol-gel, polymerized complex method (also known as Pechini method) and others to improve the problem in SSR method. Among of the above methods, polymerized complex method (PCM) offers advantages in uniformity and homogeneous atomic components of the samples and low synthetization temperature compared to SSR method.

PCM is based on the principles of sol-gel chemistry, which uses small molecule chelating ligands to generate a homogenous solution of metal/citrate complexes. Transesterification of citrate and ethylene glycol is a crucial step in the PCM as shown in Fig. 1.9. A metal salt is dissolved in water with citric acid and ethylene glycol to produce a homogenous precursor solution comprising metal-citrate chelate complexes in a conventional synthesis. This solution is heated to conduct polysterification between the citrate and ethylene glycol, producing an extensive covalent network. Lastly, the material is heated in a furnace, where the organic matrix is combusted and the ceramic product is formed.

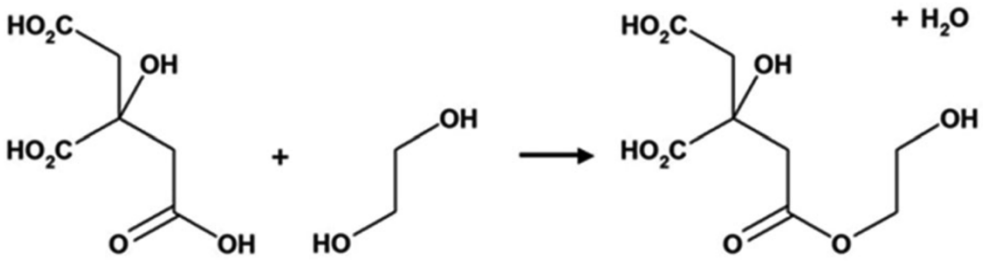


Fig. 1.9 The polyesterification between citric acid and ethylene glycol [1.53]

In this study, Eu-doped silicate phosphor was synthesized by improved PCM, which tetraethyl orthosilicate (TEOS) was used as Si based and propylene glycol (PG) as chelated agent. As TEOS have water insoluble properties. Ethanol was added to achieve smooth reaction. Fig. 1.10 shows the draft process of improved PCM in this study.

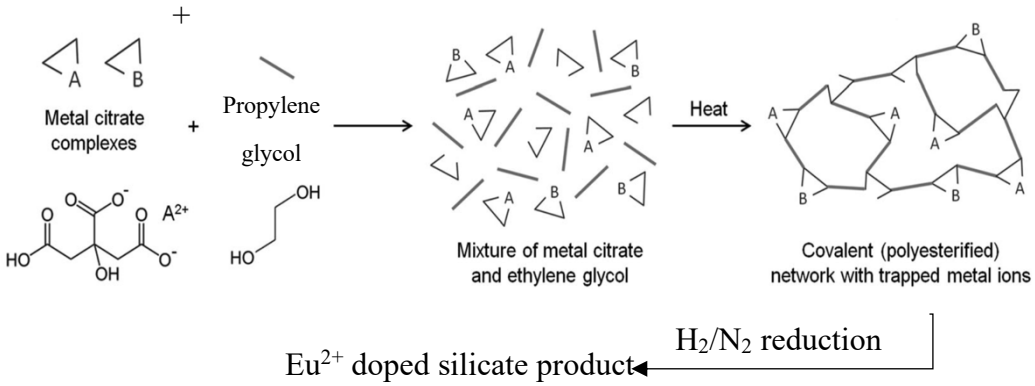


Fig. 1.10 The draft process of improved PCM of making Eu2+ doped silicate phosphor [1.53]

As general PCM has advantage in homogeneous solution, the improved PCM might show high potential in silicate phosphors. Therefore, $Sr_2SiO_4:Eu^{2+}$ and $Li_2SrSiO_4:Eu^{2+}$ phosphors were synthesized by improved PCM to produce high quality silicate phosphors. The characteristics and the properties of both silicate phosphors were investigated.

## 1.6 Scope of the thesis

In this study, $Sr_2SiO_4:Eu^{2+}$ and $Li_2SrSiO_4:Eu^{2+}$ phosphors were synthesized by improved PCM and their characteristics in terms of crystal structure, optical properties, Eu doping limitation and thermal stability were investigated. Many silicates phosphors were synthesized by conventional SSR method and only a few reports regarding the synthesis of silicate phosphors by using PCM or Pechini method. In this study, we successfully synthesized both silicate phosphors by improved PCM. Firstly, $Sr_2SiO_4:Eu^{2+}$ phosphors were synthesized as basic phosphors. $Sr_2SiO_4:Eu^{2+}$ phosphors show homogenous and good crystallinity, which indicating that improved PCM have high potential in silicate phosphors in aspect of crystallinity. As $Sr_2SiO_4:Eu^{2+}$ phosphors have α' ↔ β phase transition, it seems affect the chromaticity of emission color and performances of white LEDs application. Therefore, $Li_2SrSiO_4:Eu^{2+}$ phosphors were synthesized by Li introduction to fix the phase in the host lattice. $Li_2SrSiO_4:Eu^{2+}$ phosphors show yellow broad emission with high chemical and physical stabilities. The objectives of the research to solve the problem of low thermal stability in $YAG:Ce^{3+}$ phosphors with silicate-based phosphors system, which are synthesized by improved PCM using TEOS. The optical properties of the synthesized basic phosphors $Sr_2SiO_4:Eu^{2+}$ were investigated as basic procedure. Then, $Li_2SrSiO_4:Eu^{2+}$ phosphors were synthesized and the optical properties of the phosphors were also investigated. High thermal stability $Li_2SrSiO_4:Eu^{2+}$ yellow phosphors are targeted in this study for the high power efficiency white LEDs, which feasible replacement of $YAG:Ce^{3+}$ as yellow phosphors.

## 1.7 References


[1.1] Josephson, Matthew and Conot, Robert E. “Thomas Edison”. Encyclopedia Britannica, 7 Feb. 2021, https://www.britannica.com/biography/Thomas-Edison. Accessed 4 July 2021.

[1.2] E. F. Patrice Jelliffe, Derrick B. Jelliffe, Adverse Effects of Foods, Springer US, Boston, MA, 1982.

[1.3] K. Eto, Minamata disease, Neuropathology. 20 (2000) 14–19.

[1.4] Noriyuki Hachiya, The History and the Present of Minamata Disease —Entering the second half a century—, Jpn. Med. Assoc. J. 49 (2006) 112–118.

[1.5] A. ab Aziz, N.N.B. Othman, Z. Zakaria, Legal Control for the Safety of Cosmetic Products Application Use in Malaysia, J. HALAL Ind. Serv. 3 (2020).

[1.6] Noor Aini Bohari, Shafiquzzaman Siddiquee, Suryani Saallah, Mailin Misson, Sazmal Effendi Arshad, Electrochemical Behaviour of Real-Time Sensor for Determination Mercury in Cosmetic Products Based on PANI/MWCNTs/AuNPs/ITO, Cosmetics. 8

[1.7] Shuji Nakamura, Takashi Mukai, Masayuki Senoh, Candela-class high-brightness InGaN/AlGaN double-heterostructure blue-light-emitting diodes, Appl. Phys. Lett. 64 (1994) 1687–1689.

[1.8] M.G. Craford, Commercial Light Emitting Diode Technology, in: J. Rarity, C. Weisbuch (Eds.), Microcavities Photonic Bandgaps Phys. Appl., Springer Netherlands, Dordrecht, 1996, pp. 323–331.

[1.9] Kanji Bando, Kensho Sakano, Yasunobu Noguchi, Yoshinori Shimizu, Development of high-bright and pure-white LED lamps, J. Light Vis. Environ. 22 (1998) 2–5.

[1.10] J. K. Sheu, C. J. Pan, G. C. Chi, C. H. Kuo, L.W. Wu, C. H. Chen, S. J. Chang, Y. K. Su, White-light emission from InGaN-GaN multiquantum-well light-emitting diodes with Si and Zn codoped active well layer, IEEE Photonics Technol. Lett. 14 (2002) 450–452.

[1.11] J. K. Sheu, S. J. Chang, C. H. Kuo, Y. K. Su, L. W. Wu, Y. C. Lin, W. C. Lai, J. M. Tsai, G. C. Chi, R. K. Wu, White-light emission from near UV InGaN-GaN LED chip precoated with blue/green/red phosphors, IEEE Photonics Technol. Lett. 15 (2003) 18–20.

[1.12] Shuji Nakamura, Gerhard Fasol, The Blue Laser Diode, Springer Berlin Heidelberg, Berlin, Heidelberg, 1997.

[1.13] Volker Bachmann, Cees Ronda, Andries Meijerink, Temperature Quenching of Yellow $Ce^{3+}$ Luminescence in YAG:Ce, Chem. Mater. 21 (2009) 2077–2084.

[1.14] R.-J. Xie, N. Hirosaki, Silicon-based oxynitride and nitride phosphors for white LEDs—A review, Sci. Technol. Adv. Mater. 8 (2007) 588–600.
[1.15] R. Kasuya, A. Kawano, T. Isobe, H. Kuma, J. Katano, Characteristic optical properties of transparent color conversion film prepared from YAG:$Ce^{3+}$ nanoparticles, Appl. Phys. Lett. 91 (2007) 111916.
[1.16] Zhang Yanfang, Li Lan, Zhang Xiaosong, Xi Qun, Temperature effects on photoluminescence of YAG:$Ce^{3+}$ phosphor and performance in white light-emitting diodes, J. Rare Earths. 26 (2008) 446–449.
[1.17] P. Wang, J. Song, H. Tian, Q. Lu, D. Wang, Thermal stability of luminous YAG: Ce bulk ceramic as a remote phosphor prepared through silica-stabilizing valence of activator in air, Optoelectron. Lett. 8 (2012) 201–204.
[1.18] 水産総合研究センター, イカ研究, Fish. Res. Agensy News. 18 (2019) 1–36.
[1.19] Yu-Sheng Tang, Shu-Fen Hu, Chun Che Lin, Nitin C. Bagkar, Ru-Shi Liu, Thermally stable luminescence of $KSrPO_4$:$Eu^{2+}$ phosphor for white light UV light-emitting diodes, Appl. Phys. Lett. 90 (2007) 151108.
[1.20] Xinguo Zhang, Menglian Gong, A new red-emitting $Ce^{3+}$, $Mn^{2+}$-doped barium lithium silicate phosphor for NUV LED application, Mater. Lett. 65 (2011) 1756–1758.
[1.21] Abdelhay Aboulaich, Martyna Michalska, Raphaël Schneider, Audrey Potdevin, Jérôme Deschamps, Rodolphe Deloncle, Geneviève Chadeyron, Rachid Mahiou, Ce-Doped YAG Nanophosphor and Red Emitting $CuInS_2$/ZnS Core/Shell Quantum Dots for Warm White Light-Emitting Diode with High Color Rendering Index, ACS Appl. Mater. Interfaces. 6 (2014) 252–258.
[1.22] Hong He, Renli Fu, Yongge Cao, Xiufeng Song, Zhengwei Pan, X. Zhao, Q. Xiao, R. Li, $Ce^{3+}$→$Eu^{2+}$ energy transfer mechanism in the $Li_2SrSiO_4$:$Eu^{2+}$, $Ce^{3+}$ phosphor, Opt. Mater. 32 (2010) 632–636.
[1.23] V.P. Dotsenko, S.M. Levshov, I.V. Berezovskaya, G.B. Stryganyuk, A.S. Voloshinovskii, N.P. Efryushina, Luminescent properties of Eu2+ and Ce3+ ions in strontium litho-silicate $Li_2SrSiO_4$, J. Lumin. 131 (2011) 310–315.
[1.24] X. Zhang, H. He, Z. Li, T. Yu, Z. Zou, Photoluminescence studies on $Eu^{2+}$ and $Ce^{3+}$-doped $Li_2SrSiO_4$, J. Lumin. 128 (2008) 1876–1879.
[1.25] Y. Rao, X. Hu, T. Liu, X. Zhou, X. Zhou, Y. Li, $Pr^{3+}$-doped $Li_2SrSiO_4$ red phosphor for white LEDs, J. Rare Earths. 29 (2011) 198–201.

[1.26] L. Zhang, J. Zhang, X. Zhang, Z. Hao, G.-H. Pan, H. Wu, Site distortion in $Li_2SrSiO_4$: Influence on $Pr^{3+}$ emission and application in wLED, J. Lumin. 180 (2016) 158–162.
[1.27] Zhen Wei, Yongli Wang, Xiaobo Zhu, Jinyu Guan, Weixi Mao, JuanJuan Song, Solid state synthesis and tunable luminescence of $Li_2SrSiO_4:Eu^{2+}/Ce^{3+}$ phosphors, Chem. Phys. Lett. 648 (2016) 8–12.
[1.28] Pan Li You, Study on the Morphology and Thermal Stability of $Li_2SrSiO_4:Tb^{3+}$ Materials, Adv. Mater. Res. 989–994 (2014) 437–440.
[1.29] Thomas L. Barry, Fluorescence of $Eu^{2+}$-Activated Phases in Binary Alkaline Earth Orthosilicate Systems, J. Electrochem. Soc. 115 (1968) 1181–1184.
[1.30] Kenichi Machida, Ginya Adachi, Jiro Shiokawa, Masahiko Shimada, Mitsue Koizumi, Kaichi Suito, Akifumi Onodera, High-pressure Synthesis, Crystal Structures, and Luminescence Properties of Europium(II) Metasilicate and Europium(II)-Activated Calcium and Strontium Metasilicates, Inorg. Chem. 21 (1982) 1512–1519.
[1.31] K. Machida, G. Adachi, N. Ito, J. Shiokawa, M. Shimada, M. Koizumi, Luminescence properties for the high-pressure polymorphs of $CaSiO_3:Pb^{2+}$ and $SrSiO_3:Pb^{2+}$, Mater. Res. Bull. 17 (1982) 451–457.
[1.32] Stefan Tasch, Peter Pachler, Gundula Roth, Walter Tews, Wolfgang Kempfert, Detlef Starick, Light Source Comprising A Light-Emitting Element, United States U.S. Patent, US 6809347 B2, 1980.
[1.33] L.G. Van Uitert, Characterization of Energy Transfer Interactions between Rare Earth Ions, J. Electrochem. Soc. 114 (1967) 1048.
[1.34] D. L. Dexter, A Theory of Sensitized Luminescence in Solids, J. Chem. Phys. 21 (1953) 836–850.
[1.35] Siti Sarina Binti Nasir, Kouta Yakura, Noriyuki Horiuchi, Masaya Tsuta, Ariyuki Kato, Effect of Eu doping on room temperature phase and phase transition of $Sr_2SiO_4:Eu^{2+}$ phosphor synthesized by polymerized complex method, J. Phys. Chem. Solids. 133 (2019) 135–141.
[1.36] Siti Sarina Binti Nasir, Akihiro Tanaka, Shuto Yoshiara, Ariyuki Kato, Luminescence properties of $Li_2SrSiO_4:Eu^{2+}$ silicate yellow phosphors with high thermal stability for high-power efficiency white LED application, J. Lumin. 207 (2019) 22–28.
[1.37] David R Lide, Grace Baysinger, Swain Chemistry, Henry V Kehiaian, CRC Handbook of Chemistry and Physics, 89th edition, 2008.

[1.38] Joung Kyu Park, Mi Ae Lim, Chang Hae Kim, Hee Dong Park, Joon Taik Park, Se Young Choi, White light-emitting diodes of GaN-based $Sr_2SiO_4$:Eu and the luminescent properties, Appl. Phys. Lett. 82 (2003) 683–685.

[1.39] Y. Sun Won, S.S. Park, Density functional theory study on two-peak emission of $Eu^{2+}$ activators in $Sr_2SiO_4$, J. Phys. Chem. Solids. 71 (2010) 1742–1745.

[1.40] J.S. Kim, P.E. Jeon, Y.H. Park, J.C. Choi, H.L. Park, Color Tunability and Stability of Silicate Phosphor for UV-Pumped White LEDs, J. Electrochem. Soc. 152 (2005) H29.

[1.41] H. He, R. Fu, X. Zhang, X. Song, X. Zhao, Z. Pan, Photoluminescence spectra tuning of $Eu^{2+}$ activated orthosilicate phosphors used for white light emitting diodes, J. Mater. Sci. Mater. Electron. 20 (2009) 433–438.

[1.42] Y. Hu, W. Zhuang, J. Hao, X. Huang, H. He, Preparation mechanism and luminescence of $Sr_2SiO_4$:Eu phosphor from (Sr, Eu)$CO_3$@$SiO_2$ core-shell precursor, Open J. Inorg. Chem. 02 (2012) 6–11.

[1.43] J.H. Park, W. Ahn, Y.J. Kim, Phase formation and luminescence of $Sr_2SiO_4$:$Eu^{2+}$ nanopowders prepared by a hybrid process, Ceram. Int. 41 (2015) S734–S739.

[1.44] M. Catti, G. Gazzoni, G. Ivaldi, G. Zanini, The β ⇄ α' phase transition of $Sr_2SiO_4$. I. Order–disorder in the structure of the α' form at 383 K, Acta Crystallogr. B. 39 (1983) 674–679.

[1.45] Zhen Song, Xianlin Ding, Shanshan Yang, Feifei Du, Liu Bian, Shanghong Duan, Q.L. Liu, Thermochromic material $Sr_2SiO_4$:$Eu^{2+}$ based on displacive transformation, J. Lumin. 152 (2014) 199–202.

[1.46] M. Catti, G. Gazzoni, The β ⇄ α' phase transition of $Sr_2SiO_4$. II. X-ray and optical study, and ferroelasticity of the β form, Acta Crystallogr. B. 39 (1983) 679–684.

[1.47] Li-Cheng Ju, Chao Cai, Qiang-Qiang Zhu, Jia-Ye Tang, Lu-Yuan Hao, Xin Xu, Color tunable $Sr_2SiO_4$:$Eu^{2+}$ phosphors through the modification of crystal structure, J. Mater. Sci. Mater. Electron. 24 (2013) 4516–4521.

[1.48] Abanti Nag, T. R. N. Kutty, The light induced valence change of europium in $Sr_2SiO_4$:Eu involving transient crystal structure, J. Mater. Chem. 14 (2004) 1598–1604.

[1.49] S.K. Gupta, M.K. Bhide, R.M. Kadam, V. Natarajan, S.V. Godbole, Nanorods of white light emitting $Sr_2SiO_4$:$Eu^{2+}$ : microemulsion-based synthesis, EPR, photoluminescence, and thermoluminescence studies, J. Exp. Nanosci. 10 (2015) 610–621.

[1.50] Barbara Haferkorn, Gerd Meyer, $Li_2EuSiO_4$, ein Europium(II)-dilithosilicat: Eu[($Li_2Si$)$O_4$], Z. Für Anorg. Allg. Chem. 624 (1998) 1079–1081.

[1.51] Yoshinori Hirano, Tomoyuki Iwata, Koichi Momma, Koichiro Fukuda, Electron density distribution and crystal structure of lithium strontium silicate, $Li_2SrSiO_4$, Powder Diffr. 25 (2010) 4–8.
[1.52] 櫛田孝司, 光物性物理学, 新装版, 朝倉書店, 2010.
[1.53] A. E. Danks, S. R. Hall, Z. Schnepp, The evolution of 'sol–gel' chemistry as a technique for materials synthesis, Mater. Horiz. 3 (2016) 91–112.
[1.54] J.H. Lee, Y.J. Kim, Photoluminescent properties of $Sr_2SiO_4:Eu^{2+}$ phosphors prepared by solid-state reaction method, Mater. Sci. Eng. B. 146 (2008) 99–102.
[1.55] N. Lakshminarasimhan, U. V. Varadaraju, White-Light Generation in $Sr_2SiO_4:Eu^{2+}$, $Ce^{3+}$ under Near-UV Excitation, J. Electrochem. Soc. 152 (2005) H152–H156.
[1.56] C.-H. Hsu, R. Jagannathan, C.-H. Lu, Luminescent enhancement with tunable emission in $Sr_2SiO_4$: $Eu^{2+}$ phosphors for white LEDs, Mater. Sci. Eng. B. 167 (2010) 137–141.

# Chapter 2

# Preparation of $Sr_2SiO_4:Eu^{2+}$ silicate phosphors by improved polymerized complex method using TEOS

## 2.1 Introduction

$Sr_2SiO_4:Eu^{2+}$ silicate phosphors are one of the silicate-based phosphors possesses promising luminescent materials with good properties for white LEDs and thermochromic application [2.1]. This is due to two crystalline phases in have unique properties, which have two crystalline structures $Sr_2SiO_4$ host lattice; (i) high temperature α' phase (orthorhombic) with space group Pmnb which is applicable in white LED application and (ii) low temperature β phase (monoclinic) with space group $P2_1/n$ which is applicable in thermochromic application. M. Catti et al. reported that the phase transition temperature between α' ↔ β phases is at 85 °C [2.2–2.4].The most challenging task is to obtain and synthesized pure β - $Sr_2SiO_4$ at room temperature as the only small amount of impurities or doping effect the crystallinity of the host lattice, leading the samples easily change to α' phase below 85 °C. According to J. Cu et al., only small amount of Ba doping (1%) is used to stabilize the $Sr_2SiO_4$ host lattice and becomes α' - $Sr_2SiO_4$ [2.1]. Usually, Eu doping are used to synthesis the luminescent materials, which is similar system was putting impurities into the host lattice, affecting the crystallinity and phase of the samples. According to previous reports, β - $Sr_2SiO_4:Eu^{2+}$ phosphors were mostly synthesized by conventional SSR method, which required high temperature about 1500 °C above [2.5–2.10] . Other than that, combustion, sol-gel/Pechini and co-precipitation methods are also several methods that using solution route, which are good in controlling dopants to synthesis the samples [2.11,2.12]. However, only α' phase or mixture of α' + β phases (α' phase

are dominant) of the samples can be obtained from these methods. Therefore, improved PCM were demonstrated to synthesize $Sr_2SiO_4:Eu^{2+}$ phosphors in this study.

## 2.2 Experimental procedure

$Sr_2SiO_4:Eu^{2+}$ phosphors were synthesized by improved PCM[2.13,2.14], which using TEOS[2.15] and advantages in uniformity of atomic components of the samples and low synthetization temperature, were demonstrated to synthesize $Sr_2SiO_4:Eu^{2+}$ phosphors as basic phosphors. HCl and $HNO_3$ dependence, reduction/sintering temperature dependence and Eu concentration dependence of $Sr_2SiO_4:Eu^{2+}$ phosphors were investigated. The crystal structure and optical properties of the samples were identified by XRD and PL spectra measurement. Fig. 2.1 below shows the synthesis flowchart of $Sr_2SiO_4:Eu^{2+}$ phosphors.

Firstly, $SrCO_3$ (kojundo, 99.9%) and $Eu_2O_3$ (kojundo, 99.9%) as starting materials were weighed stoichmetrically with different Eu concentration. Eu concentration was varied from 1%, 3%, 5%, 10% and 20%. The starting materials were dissolved in $HNO_3$ or HCl aqueous solution (mixture of 2 ml of HCl or $HNO_3$ and 5 ml of water) for comparison. Then citric acid (nacalai, 99.0%) was added as chelated agent and the solution were heated and stirring at 80 °C for 24 h. After that, TEOS (nacalai, 95.0%) were used for Si source for the phosphors. As TEOS insoluble in water, ethanol was added to prevent cloudy solution. The propylene glycol (PG) was added for the gelation process while the solution was stirred at 120 °C for 3h, where TEOS and PG lead to dehydration and esterification reaction between carboxyl group of chelated complex and hydroxyl group of polymerization agent, resulting in formation of gel (polymers). The formed gel was dried at 250 °C for 30 min and decomposed at 400 °C for 1h by electric furnace to remove organic materials in the gel and formed precursors. The precursors were calcined by air at 1000 °C for 3h and lastly, the samples were undergoing $H_2/N_2$ (5% $H_2$/95% $N_2$) reduction at different reduction/sintering temperature for 3h. The

reduction/sintering temperature were set up from 900 °C, 1150 °C and 1400 °C temperature range.

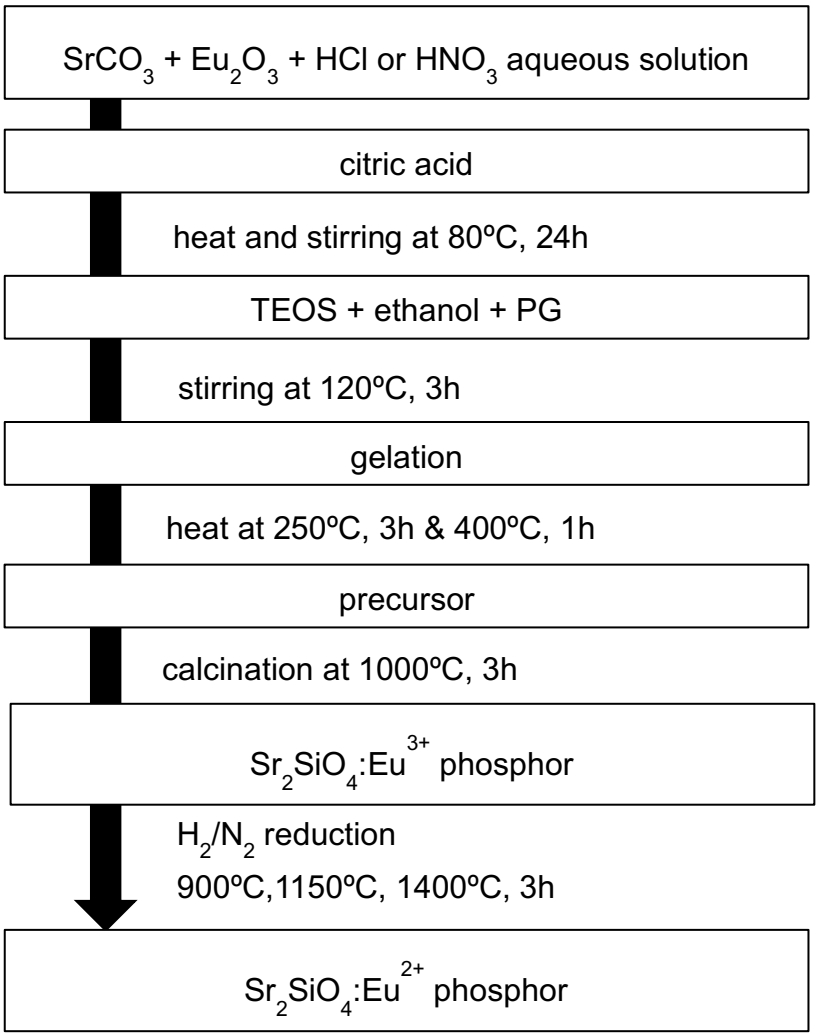


Fig. 2.1 Synthesis flowchart of $Sr_2SiO_4:Eu^{2+}$ phosphors

The crystal structures of the prepared phosphors were investigated by X-ray diffraction (XRD) spectrometer by using Cu-Kα as X-ray source (Shimadzu, XRD-7000, λ=1.541838 Å, 40 kV, 30 mA. The optical properties or photoluminescence spectra (PL) of the samples were measured by photoluminescence and a spectrometer (Andor, Shamrock SR-163, f=160 mm) equipped with CCD as a detector (Andor, iDus DV-420A-OE). He–Cd laser (KIMMON KOHA, IK3202R-D, 25 mW, 325 nm) was used as excitation light source.

Table 2.1 XRD specifications

| Specifications | Setting value |
|---|---|
| Voltage | 40kV |
| Current | 30mA |
| Diverging slit | 1.0° |
| Scattering slit | 1.0° |
| Light receiving slit | 0.15mm |
| Step width | 0.01° |
| Scan speed | 4.00°/min |
| Integration number | 1 |
| Measurement range | 10～80° |

## 2.3 Results and discussions

### 2.3.1 HCl and $HNO_3$ dependence

The crystal structure of synthesized $Sr_2SiO_4:Eu^{2+}$ phosphors are shown in Fig.2.2 below. The international center for diffraction data (ICDD) shows the significant peaks α' and β - $Sr_2SiO_4$ around 27 ° (112) and 32.5° (301) respectively. The phase of the samples can be easily distinguished by these significant peaks. From Fig. 2.2, when the samples were calcined at 1000 °C by air after the pyrolysis at 400 °C, α'- $Sr_2SiO_4:Eu^{2+}$ phosphors can be observed. After the samples went through reduction process under $H_2/N_2$ ambient at 1150 °C, peaks of α'- $Sr_2SiO_4:Eu^{2+}$ phosphors can be observed for the samples using $HNO_3$. Meanwhile, peaks of β - $Sr_2SiO_4:Eu^{2+}$ phosphors can be observed for the samples using HCl. This indicates that β - $Sr_2SiO_4:Eu^{2+}$ phosphors can be synthesized by using HCl compared to $HNO_3$ although in the same reduction temperature due to the presence of flux during the preparation of the samples. $SrCl_2$ peaks were slightly observed when the samples were heated in the air and gradually

decrease when undergoes reduction/sintering process at 1150 °C. $SrCl_2$ can be formed from the reaction between starting materials $SrCO_3$ and HCl and expected to act as flux during reduction process. The presence of flux leads to good crystallinity of the samples, which β- $Sr_2SiO_4:Eu^{2+}$ phosphors can be synthesized by improved PCM using HCl [2.1,2.16]. Meanwhile, $Sr(NO_3)_2$, which is formed from the reaction between starting material $SrCO_3$ and $HNO_3$ for the samples prepared with $HNO_3$, might acts as flux. However, it is possible that $Sr(NO_3)_2$ flux is decomposed at 1150 °C as the melting point of $Sr(NO_3)_2$ (570 °C) is lower than $SrCl_2$ (870 °C), resulting in the formation of α'- $Sr_2SiO_4:Eu^{2+}$ phosphors . As shown in Fig. 2.2, no $Sr(NO_3)_2$ peaks can be observed when the samples were heated at 1000 °C and after reduction process at 1150 °C. It can be concluded that the presence of flux is one of the significant factors for the synthetization of β- $Sr_2SiO_4:Eu^{2+}$ phosphors.

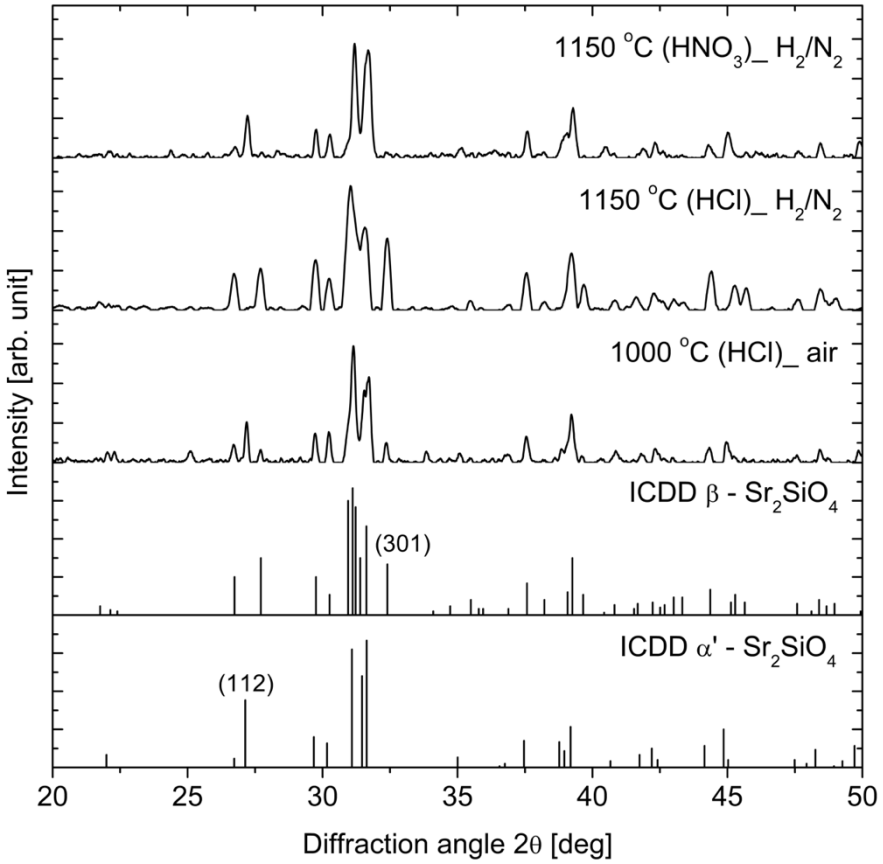


Fig. 2.2 XRD patterns of $Sr_2SiO_4:Eu^{2+}$ phosphors by using $HNO_3$ and HCl as comparison

Fig. 2.3 shows the PL spectra of prepared $Sr_2SiO_4:Eu^{2+}$ phosphors by using HCl and $HNO_3$ at the same reduction temperature (1150 °C) for comparison. As shown in Fig. 2.3, all the samples show green emission bands and different emission peaks can be observed. The samples prepared by using HCl show β phase emission peak around 540 nm and show higher PL intensity. Meanwhile, α' phase emission peak around 550 nm can be observed for the samples prepared by using $HNO_3$, which show lower PL intensity compared to the samples were prepared using HCl. This is assigned to the presence and function of the flux in the samples, where $Sr(NO_3)_2$ flux is completely vaporized during reduction process at 1150 °C for the samples prepared using $HNO_3$ and effect the crystallinity of the samples, resulting to form α'- $Sr_2SiO_4:Eu^{2+}$ phosphors. For the samples prepared using HCl, $SrCl_2$ flux still functioning during reduction process at 1150 °C, which lead to good crystallinity and can synthesize β-$Sr_2SiO_4:Eu^{2+}$ phosphors. As there are two $Sr^{2+}$ sites in the $SrSiO_4$ host lattice (9-coordinated and 10-coordinated), $Eu^{2+}$ ions will substitute into these two different $Sr^{2+}$ sites to form different emission bands, resulting of different in peak emission wavelength.

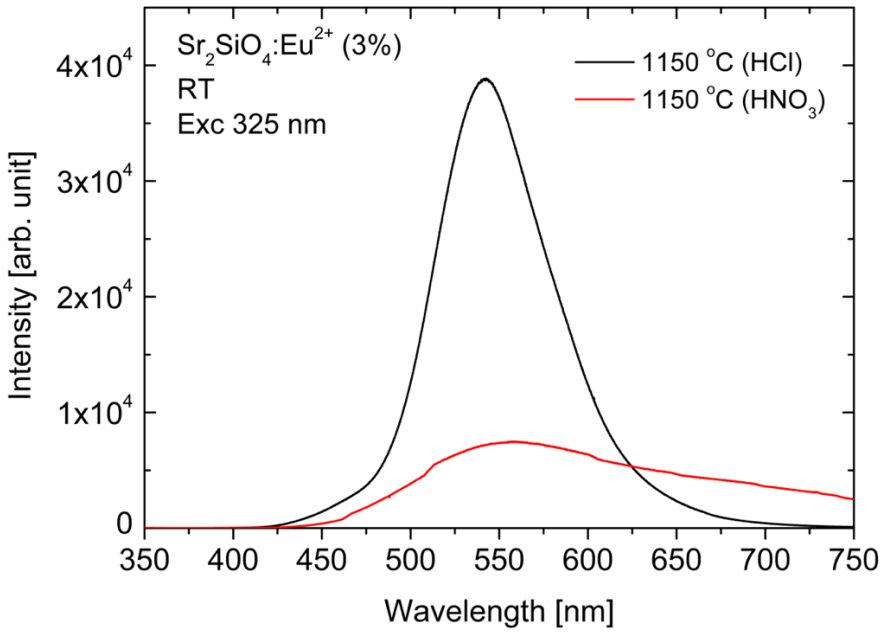


Fig. 2.3 PL spectra of $Sr_2SiO_4:Eu^{2+}$ phosphors by using $HNO_3$ and HCl as comparison

### 2.3.2 Reduction/sintering temperature dependence

Fig. 2.4 show the XRD patterns of prepared $Sr_2SiO_4:Eu^{2+}$ (3%) phosphors with different sintering temperatures. The peaks of α' and β of the samples were determined by the significant peaks from ICDD data of α' and β - $Sr_2SiO_4$, which are around 27° (112) and 32.5° (301), respectively. The phase ratio of the prepared samples can be estimated comparing intensities between these significant peaks. The results show the samples prepared at 900 °C sintering temperature show β - $Sr_2SiO_4$ as dominant co-existed with α' phase and also small weak peaks of $SrCl_2$. As sintering temperature increases, the samples prepared at 1150 °C show almost completely β - $Sr_2SiO_4$ and the residual $SrCl_2$ peaks gradually decreases. The samples prepared at highest temperature, 1400 °C appears completely α' - $Sr_2SiO_4$ and the residual $SrCl_2$ peaks completely disappeared.

As mentioned in section 2.3.1, these residual $SrCl_2$ peaks are originated from the reaction between $SrCO_3$ and HCl under reduction atmosphere because these $SrCl_2$ lines could not be observed from the sample before reduction process. The residual $SrCl_2$ is expected to act as flux during reduction process due to higher reduction temperature than melting point of $SrCl_2$ (874 °C). Weak $SrCl_2$ lines also can be observed at 1150 °C and diminished at 1400 °C. $SrCl_2$ seem to be vaporized and disappeared completely at 1400 °C because the boiling point of $SrCl_2$ is 1250 °C. L.C. Ju et al reported that β - $Sr_2SiO_4:Eu^{2+}$ phosphors can be synthesized at 1500 °C by conventional SSR without flux [2.1]. It indicates that high temperature is required to obtain β - $Sr_2SiO_4:Eu^{2+}$ phosphors with high crystallinity. In this study, β - $Sr_2SiO_4:Eu^{2+}$ phosphors were successfully synthesized at 1150 °C by improved PCM using HCl, which lower temperature than previous report [2.1]. From this study, the presence of flux plays important role in the synthesis of β - $Sr_2SiO_4:Eu^{2+}$ phosphors at low reduction temperature, because flux leads to the good and high crystallinity of the samples.

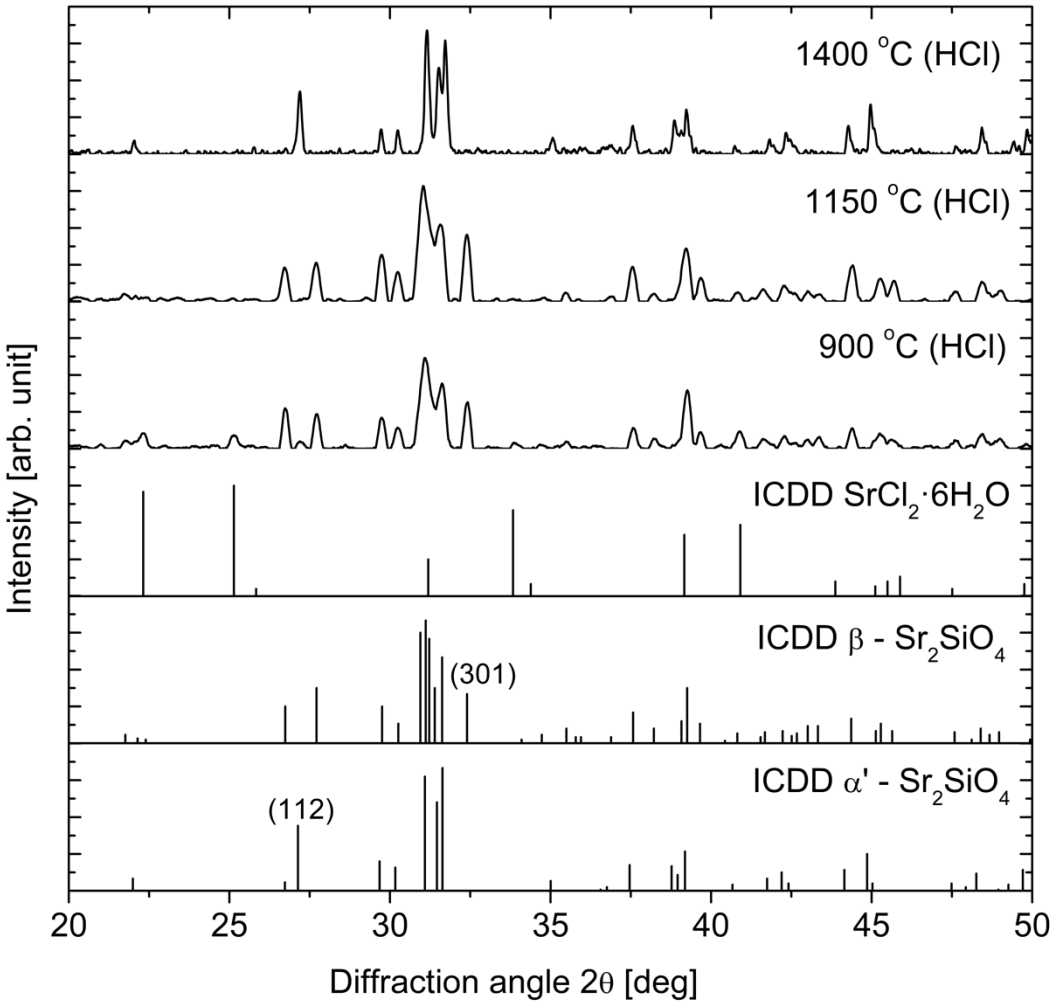


Fig. 2.4 The XRD patterns of $Sr_2SiO_4:Eu^{2+}$ (3%) phosphors by improved PCM using HCl with different sintering temperatures

The optical properties of $Sr_2SiO_4:Eu^{2+}$ (3%) phosphors were also investigated by PL measurements. From Fig. 2.5, PL spectra of the samples prepared at 900 °C and 1150 °C show green emission bands around 540 nm, which show β phase emission, where the samples prepared at 1150 °C show the highest PL intensity among all the samples. In other hands, the lowest PL intensity can be observed for the samples prepared with highest temperature, 1400 °C and show emission peak around 560 nm, which show α' phase emission. The wavelengths of these PL bands are interrelated to the wavelength of α' and β phases, which

stated from previous reports[2.1,2.17,2.18]. These wavelengths support the phase identification by XRD in previous chapter. Therefore, it is known that the optimum sintering temperature for β - $Sr_2SiO_4:Eu^{2+}$ (3%) phosphors is 1150 °C, which show almost pure β phase with high PL intensity.

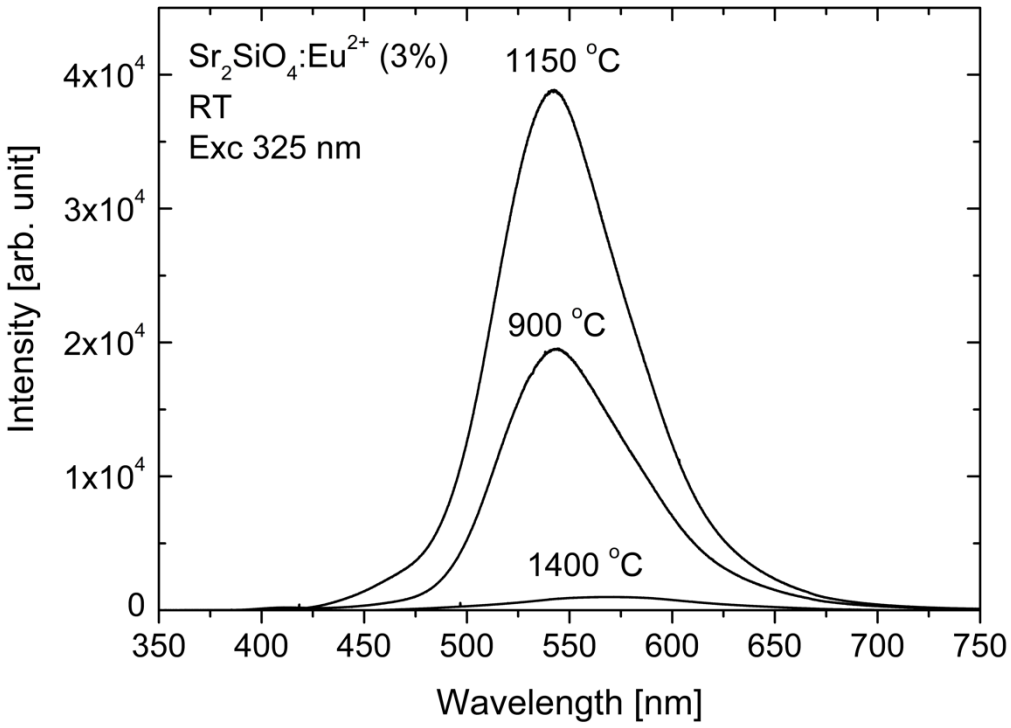


Fig. 2.5 The PL spectra of $Sr_2SiO_4:Eu^{2+}$ (3%) phosphors by improved PCM using HCl with different sintering temperatures

### 2.3.3 Eu concentration dependence

Eu concentration dependence of $Sr_{2(1-x)}Eu_{2x}SiO_4$ phosphors were investigated by XRD and PL spectra. In this section, $Sr_{2(1-x)}Eu_{2x}SiO_4$ phosphors with different Eu concentrations ($x$ = 0.01, 0.03, 0.05, 0.1, 0.2) were synthesized by improved PCM using HCl at 1150 °C $H_2/N_2$ reduction temperature, which is the optimum sintering temperature from the previous section. Although the samples contain different phase of $SrCl_2$ from previous section, it can be neglected for the samples reduced at 1150 °C as it appears in only quite small and weak. Therefore, the nominal x will be dealt with as actual Eu concentration, where $x$ was determined by molar ratio of starting materials.

The crystal structure of $Sr_{2(1-x)}Eu_{2x}SiO_4$ phosphors with different Eu concentrations were investigated and shown in Fig. 2.6. The phase of all the samples were identified by the significant line intensities (301) and (112) of α' and β -$Sr_2SiO_4$ from ICDD, which are similar from previous section. From Fig. 2.6, the samples with 1% and 3% Eu concentration show the samples are in almost β phase. The samples with 5% Eu concentration also show β phase as dominant but co-existed with weak α' phase. Meanwhile, the XRD patterns of the samples with 5% and 10% Eu concentration shows α' - $Sr_2SiO_4:Eu^{2+}$ phosphors. These XRD results indicates that almost pure β - $Sr_2SiO_4:Eu^{2+}$ phosphors samples can be synthesized with low Eu concentration, which are 1% and 3% Eu concentration.

From the previous reports, $Sr_2SiO_4$ phosphors show β phase by Ba doping up to 0.5% as mentioned in section 2.1[2.1]. According to R.D. Shannon, ionic radii of $Sr^{2+}$, $Eu^{2+}$ and $Ba^{2+}$ at 8-folded coordinates are 126 pm, 125 pm and 142 pm, respectively [2.19]. It is stated that ionic radius of $Sr^{2+}$ and $Eu^{2+}$ are almost similar. Meanwhile, the ionic radius of Ba is much bigger than $Sr^{2+}$. It indicates the Eu substitution on Sr sites bring small strain on the host lattice compared to Ba substitution, which consequently leading to the difference of critical Eu concentration. In this study, β-$Sr_2SiO_4$ can be observed until 5% Eu doping, which is much

higher than 0.5% Ba doping. Besides that, there are no reports regarding that β- $Sr_2SiO_4$ can be observed up to Eu concentration of 5%. This high critical concentration is assigned to improved PCM with flux which has the advantage to obtain uniform dopant distribution.

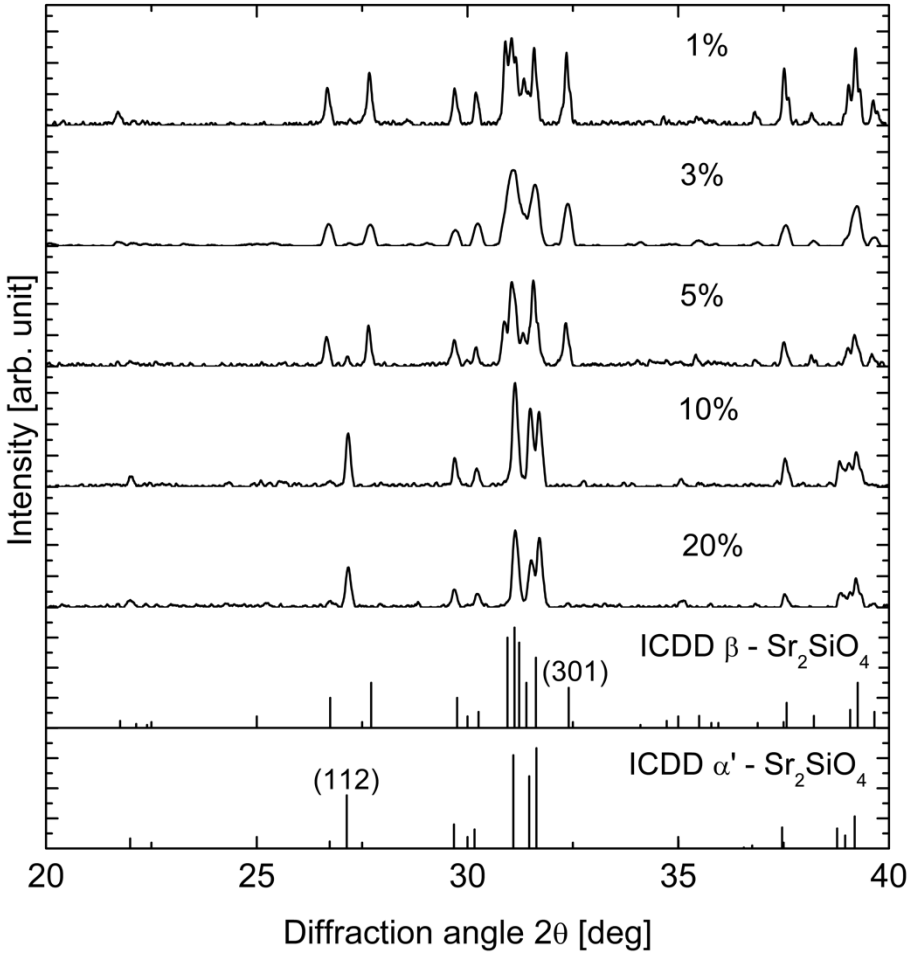


Fig. 2.6 The XRD patterns of $Sr_2SiO_4:Eu^{2+}$ phosphors by improved PCM using HCl at 1150 °C with different Eu concentrations

After the investigation of crystal structure of all the samples, the optical properties of $Sr_{2(1-x)}Eu_{2x}SiO_4$ phosphors ($x$ = 0.01, 0.03, 0.05, 0.1, 0.2) were also investigated. PL spectra in Fig. 2.7 show that there are two emission bands around 470 nm and 540 nm can be observed for the samples with 1%, 3% and 5% Eu concentration, which are β phase, where the samples with 3% Eu concentration show the highest PL intensity among all the samples. These emission bands represents β-Eu(1) and β-Eu(2), respectively. On the other hands, weak band around 490 nm and strong emission bands around 570 nm can be observed for the samples with 10% and 20% Eu concentrations, where low PL intensity can be observed. These aforementioned emission bands represents as α'-Eu(1) and α'-Eu(2), respectively. These four bands are attributed to the $4f^65d^1 \rightarrow 4f^7$ transition in $Eu^{2+}$ ions [2.20] and can be used for the identification α' and β phases of the samples. It is known that $Eu^{2+}$ ions will substitute in two different $Sr^{2+}$ sites in both α' and β phases $Sr_2SiO_4$. There are two types of bands, which are short wavelength emission band, Eu(1) and long wavelength emission band, Eu(2) [2.1]. These bands are known to be different depending on the α' and β phases. Table 2.2 shows the emission bands from both Eu(1) and Eu(2).

Table. 2.2 The emission bands from Eu(1) and Eu(2)

| Coordinated site | 9-coordinated Sr site (weak crystal field) | 10-coordinated Sr site (strong crystal field) |
|---|---|---|
| Emission bands | Eu (1) | Eu(2) |
| β phase | 470 nm | 540 nm |
| α' phase | 490 nm | 570 nm |

From PL spectra in Fig. 2.7, the concentration quenching can be observed at the main emission band β-Eu(2) and shift to α'-Eu(2) as the Eu concentration increases. The emission bands β-Eu(1) show sudden Eu concentration quenching at 5%. In this study, 3% is the most optimum Eu doping concentration for the synthesis of β-$Sr_2SiO_4$:$Eu^{2+}$ phosphors because of the highest intensity and almost pure β phase can be obtained from both XRD and PL results.

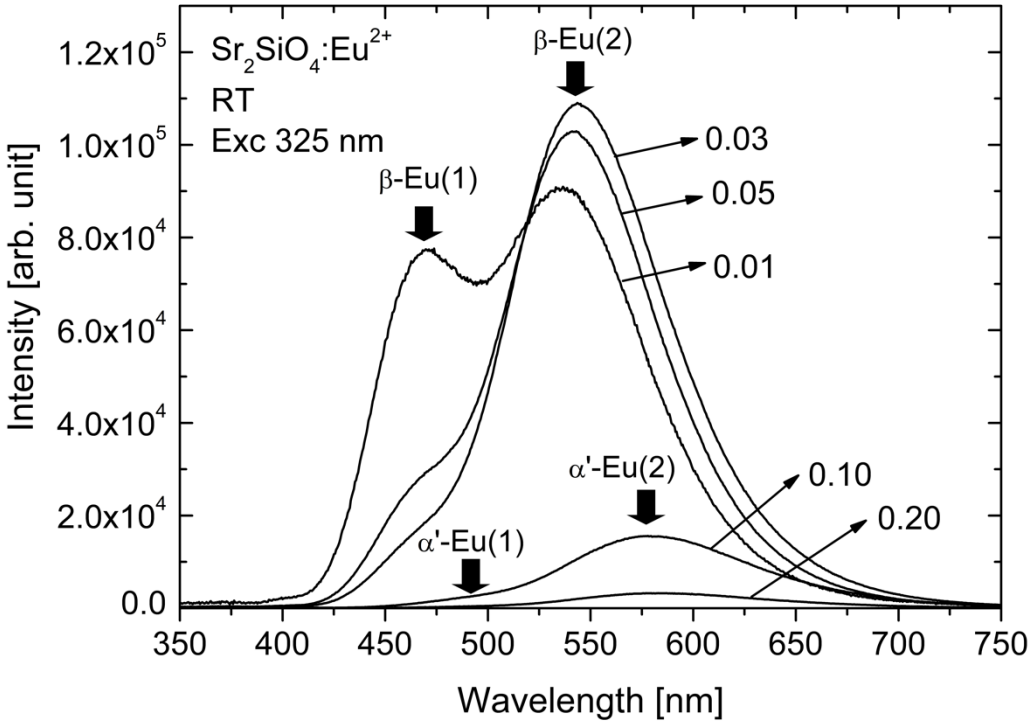


Fig. 2.7 The PL spectra of $Sr_2SiO_4$:$Eu^{2+}$ phosphors by improved PCM using HCl at 1150 °C with different Eu concentrations

## 2.4 Conclusions

In this study, $Sr_2SiO_4:Eu^{2+}$ phosphors were synthesized by improved PCM, which using TEOS. There are three main dependences were investigated; HCl and $HNO_3$ dependence, reduction/sintering temperature and Eu concentration. For HCl and $HNO_3$ dependence, the reduction/sintering temperature was set to 1150 °C and 3% Eu concentration for both samples. From XRD results, β - $Sr_2SiO_4:Eu^{2+}$ lines can be observed for the samples were prepared by using HCl. Meanwhile, α'- $Sr_2SiO_4:Eu^{2+}$ lines can be observed for the samples were prepared by using $HNO_3$. This is due to the presence of $SrCl_2$ and $Sr(NO_3)_2$ as flux during reduction process, which lead to good crystallinity of the samples. As the boiling point of $Sr(NO_3)_2$ is lower than $SrCl_2$, $Sr(NO_3)_2$ were possibly completely vaporized at 1150 °C reduction temperature, which affect the crystallinity of the samples, resulting to the formation α'-$Sr_2SiO_4:Eu^{2+}$ phosphors. Besides that, PL spectra of all the samples show green emission bands with different emission peaks, which are around 540 nm and 550 nm for the samples prepared using HCl and $HNO_3$ respectively. This is due to the substitution of $Eu^{2+}$ into two different $Sr^{2+}$ sites in the $Sr_2SiO_4$ in the host lattice, resulting the different emission wavelength. The results show that the samples were prepared by using HCl can synthesize β - $Sr_2SiO_4:Eu^{2+}$ (3%) phosphors at 1150 °C reduction temperature compared to $HNO_3$.

After that, the sintering temperature dependence and Eu concentration dependence of $Sr_2SiO_4:Eu^{2+}$ phosphors were investigated. Firstly, $Sr_2SiO_4:Eu^{2+}$ (3%) phosphors with different sintering temperature were synthesized by improved PCM using HCl. The XRD patterns shows the samples prepared with 900 °C shows β phase is dominant co-existed with the residual of $SrCl_2$ peaks. As the sintering temperature increases to 1150 °C, the samples show almost β phase and residual $SrCl_2$ were gradually disappeared. Then, the samples show completely α' phase and $SrCl_2$ peaks were completely diminished at 1400 °C. Therefore, the optimum sintering temperature for β phase $Sr_2SiO_4:Eu^{2+}$ phosphors is at 1150 °C.

For Eu concentration dependence, $Sr_{2(1-x)}Eu_{2x}SiO_4$ phosphors with different Eu concentrations were synthesized at 1150 °C by improved PCM using HCl. The XRD patterns show that the samples with 1% and 3% Eu concentration indicate almost β phase, while 5% Eu concentration indicate β phase as dominant co-existed with small amount of α' phase. As the Eu concentration increases to 10% and 20%, both samples show completely α' phase. The PL spectra of the samples with 1%, 3% and 5% show two emission bands around 450 nm (β-Eu(1)) and 540 nm (β-Eu(2)), which indicating the β phase emission. The highest PL intensity can be observed for the samples with 3% Eu concentration. Eu concentration quenching occurs at 5% for both β-Eu(1) and β-Eu(2) emission bands. Meanwhile, The PL spectra of the samples with 10% and 20% show weak emission bands around 470 nm (α'-Eu(1)) and 560 nm (α'-Eu(2)), which indicating the α' phase emission. Therefore, the optimum Eu concentration for the synthesis of β-$Sr_2SiO_4:Eu^{2+}$ phosphors is 3% because of the highest PL intensity. From the results above, improved PCM was successfully demonstrated to synthesize β - $Sr_2SiO_4:Eu^{2+}$ phosphors at lower temperature and higher Eu concentration.

## 2.5 References


[2.1] L.-C. Ju, C. Cai, Q.-Q. Zhu, J.-Y. Tang, L.-Y. Hao, X. Xu, Color tunable $Sr_2SiO_4:Eu^{2+}$ phosphors through the modification of crystal structure, J. Mater. Sci. Mater. Electron. 24 (2013) 4516–4521.

[2.2] M. Catti, G. Gazzoni, G. Ivaldi, Structures of twinned β-$Sr_2SiO_4$ and of α'-$Sr_{1.9}Ba_{0.1}SiO_4$, Acta Crystallogr. C. 39 (1983) 29–34.

[2.3] M. Catti, G. Gazzoni, G. Ivaldi, G. Zanini, The β ⇄ α' phase transition of $Sr_2SiO_4$. I. Order–disorder in the structure of the α' form at 383 K, Acta Crystallogr. B. 39 (1983) 674–679.

[2.4] M. Catti, G. Gazzoni, The β ⇄ α' phase transition of $Sr_2SiO_4$. II. X-ray and optical study, and ferroelasticity of the β form, Acta Crystallogr. B. 39 (1983) 679–684.

[2.5] H. He, R. Fu, X. Zhang, X. Song, X. Zhao, Z. Pan, Photoluminescence spectra tuning of $Eu^{2+}$ activated orthosilicate phosphors used for white light emitting diodes, J. Mater. Sci. Mater. Electron. 20 (2009) 433–438.

[2.6] Le Zhang, Zhou Lu, Pengde Han, Jiajia Lu, Naicen Xu, Lixi Wang, Qitu Zhang, The Evolution and Role of $NH_4Cl$ Flux Used to Synthesize $Sr_2SiO_4:Dy^{3+}$ Phosphor by Solid-State Reaction Method, J. Am. Ceram. Soc. 95 (2012) 1–7.

[2.7] Sun Xiaoyuan, Zhang Jiahua, Zhang Xia, Luo Yongshi, Wang Xiaojun, A green-yellow emitting β- $Sr_2SiO_4:Eu^{2+}$ phosphor for near ultraviolet chip white-light-emitting diode, J. Rare Earths. 26 (2008) 421–424.

[2.8] N. Lakshminarasimhan, U. V. Varadaraju, White-Light Generation in $Sr_2SiO_4:Eu^{2+}$, $Ce^{3+}$ under Near-UV Excitation, J. Electrochem. Soc. 152 (2005) H152–H156.

[2.9] C.-H. Hsu, R. Jagannathan, C.-H. Lu, Luminescent enhancement with tunable emission in $Sr_2SiO_4:Eu^{2+}$ phosphors for white LEDs, Mater. Sci. Eng. B. 167 (2010) 137–141.

[2.10] J.H. Lee, Y.J. Kim, Photoluminescent properties of $Sr_2SiO_4:Eu^{2+}$ phosphors prepared by solid-state reaction method, Mater. Sci. Eng. B. 146 (2008) 99–102.

[2.11] J.K. Han, M.E. Hannah, A. Piquette, G.A. Hirata, J.B. Talbot, K.C. Mishra, J. McKittrick, Structure dependent luminescence characterization of green–yellow emitting $Sr_2SiO_4:Eu^{2+}$ phosphors for near UV LEDs, J. Lumin. 132 (2012) 106–109.

[2.12] A. E. Danks, S. R. Hall, Z. Schnepp, The evolution of 'sol–gel' chemistry as a technique for materials synthesis, Mater. Horiz. 3 (2016) 91–112.

[2.13] Hiroki Komagata, Riku Kato, Ariyuki Kato, Synthesis of Zr-based perovskite-type alloy phosphors by polymerized complex method, Jpn. J. Appl. Phys. 53 (2014) 02BC08.

[2.14] K. Taniguchi, T. Honda, A. Kato, Eu concentration dependence of luminescent properties of $Sr_{1-x}EuxGa_2S_4$ phosphors synthesized by polymerized complex sulfurization method, Opt. Mater. 35 (2013) 1993–1996.

[2.15] Siti Sarina Binti Nasir, Akihiro Tanaka, Shuto Yoshiara, Ariyuki Kato, Luminescence properties of $Li_2SrSiO_4:Eu^{2+}$ silicate yellow phosphors with high thermal stability for high-power efficiency white LED application, J. Lumin. 207 (2019) 22–28.

[2.16] Siti Sarina Binti Nasir, Kouta Yakura, Noriyuki Horiuchi, Masaya Tsuta, Ariyuki Kato, Effect of Eu doping on room temperature phase and phase transition of $Sr_2SiO_4:Eu^{2+}$ phosphor synthesized by polymerized complex method, J. Phys. Chem. Solids. 133 (2019) 135–141.

[2.17] S.K. Gupta, M.K. Bhide, R.M. Kadam, V. Natarajan, S.V. Godbole, Nanorods of white light emitting $Sr_2SiO_4:Eu^{2+}$ : microemulsion-based synthesis, EPR, photoluminescence, and thermoluminescence studies, J. Exp. Nanosci. 10 (2015) 610–621.

[2.18] Abanti Nag, T. R. N. Kutty, The light induced valence change of europium in $Sr_2SiO_4:Eu^{2+}$ involving transient crystal structure, J. Mater. Chem. 14 (2004) 1598–1604.

[2.19] R.D. Shannon, Revised Effective Ionic Radii and Systematic Studies of Interatomie Distances in Halides and Chaleogenides, Acta Crystallogr. Sect. A. A32 (1976) 751–767.

[2.20] Y. Sun Won, S.S. Park, Density functional theory study on two-peak emission of Eu2+ activators in $Sr_2SiO_4$, J. Phys. Chem. Solids. 71 (2010) 1742–1745.

# Chapter 3

# Thermal effect on phase transition (α' ↔ β phase) of $Sr_2SiO_4:Eu^{2+}$ phosphors

## 3.1 Introduction

Thermal stability is one of the crucial factors to consider for white LEDs application and thermochromic application. In this chapter, the thermal effects on the phase transition of β-$Sr_2SiO_4:Eu^{2+}$ phosphors were identified by XRD and PL. From Chapter 2, it is known that in order to synthesis pure β phase $Sr_2SiO_4:Eu^{2+}$ phosphors, the optimum conditions for sintering temperature and Eu concentration are 1150 °C and 3% respectively. Phase transition and thermal hysteresis of the samples prepared by SSR were investigated from previous report [3.1]. However, the results were analysed qualitatively and the measured temperature range was still inadequate to discuss the phase transition. In this chapter, temperature dependence of XRD and PL of β - $Sr_2SiO_4:Eu^{2+}$ (3%) phosphors synthesized via improved PCM were analysed quantitatively. As the improved PCM using TEOS were successfully demonstrated in previous chapter, phase transition can be analysed precisely due to the good crystallinity of the samples. Therefore, the influence of Eu doping on the phase transition and thermal hysteresis were investigated.

## 3.2 Experimental procedure

Thermal effect or temperature dependence of the crystal structure of β - $Sr_2SiO_4:Eu^{2+}$ (3%) phosphors were investigated by XRD characterization. Similar XRD machine is used from previous chapter 2. Firstly, the samples were placed into metal sample holder and set up onto a hot plate (AS ONE, HHP- 170D). The height of the sample holder was adjusted by a laboratory jack to ensure the X-ray can be diffracted well on the surface of the samples. The temperatures of the hot plate were set up from 30 °C–110 °C and the temperature of the samples was monitored by a thermocouple thermometer. From the XRD results, the volume ratio of β phase in the samples were estimated by calculation. The detailed calculation of the volume ratio of α' and β phase of the samples were explained in the next section (section 3.3). To investigate the PL spectra of β - $Sr_2SiO_4:Eu^{2+}$ (3%) phosphors, the samples were set up on a soldering iron and temperature was controlled from 30 °C to 200 °C by a programmable temperature controller (RKC, PF900) equipped with single phase power regulator (RKC, THV-1). Then, the PL spectra of the samples for each temperature (30 °C to 200 °C) were measured by spectrometer similar in chapter 2. He–Cd laser (chapter 2) was used as excitation light source. The excitation wavelength of 325 nm is close to the reported peak wavelength of PL excitation (PLE) band of $Sr_2SiO4:Eu^{2+}$ phosphors [3.2].

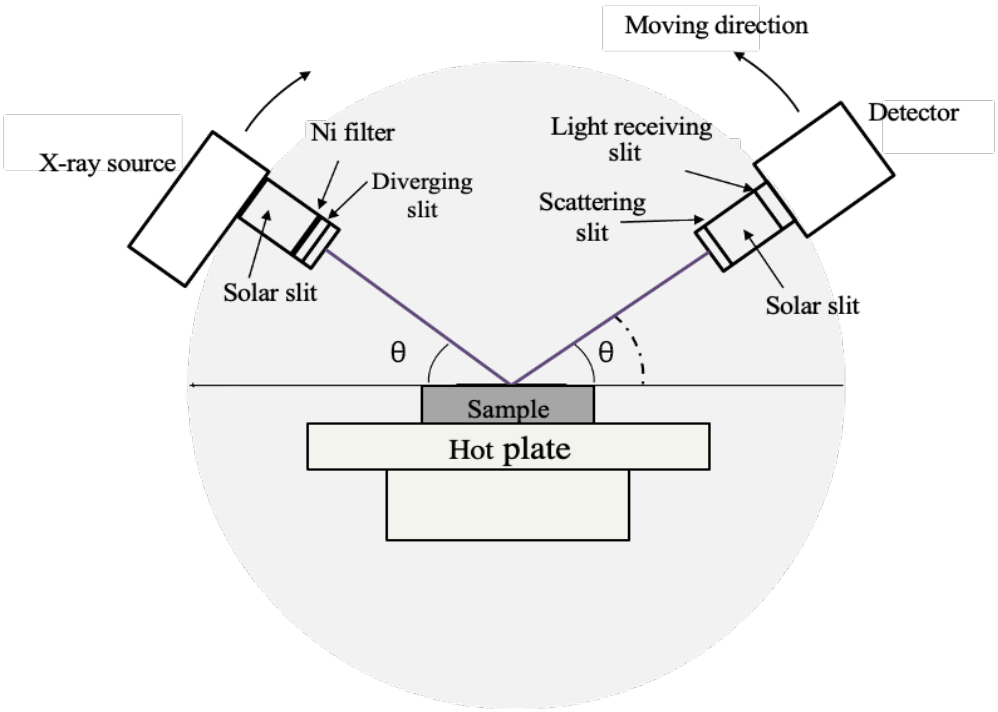


Fig. 3.1 Schematic diagram of temperature dependence by XRD

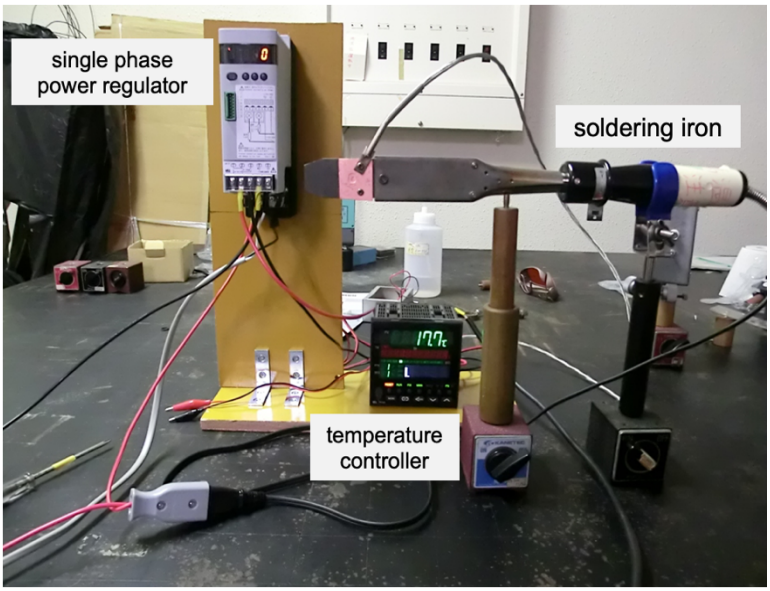


Fig. 3.2 Temperature control system for PL

## 3.3 Results and discussion

### 3.3.1 Temperature dependence of XRD

Temperature dependence of crystal structure of $Sr_2SiO_4:Eu^{2+}$ (3%) phosphors were shown in Fig. 3.3. The heating and cooling temperature range is from 30 °C to 110 °C and vice versa. At the beginning, the XRD patterns show that the samples were β - $Sr_2SiO_4$ phase at 30 °C. The β (301) line gradually decreases and the α' (112) line can be observed over 80 °C as temperature increases. Then, the intensity of α' line gradually increases as temperature reached at 110 °C with the residual amount of β phase. From the Fig. 3.3(a), phase transition from β to α' phase can be observed starting from 80 °C. However, the samples show incomplete α' phase with the mixture of residual amount of β phase, which is due to the limitation of our hot plate equipment in this study, where the maximum temperature can only be set up until 110 °C. For cooling process, where the temperature decreases from 110 °C to 30 °C, the intensity of α' line gradually decrease and the intensity of β line gradually increases around 70 °C. At the lowest temperature (30 °C), the samples show almost β phase (Fig. 3.3(b)).

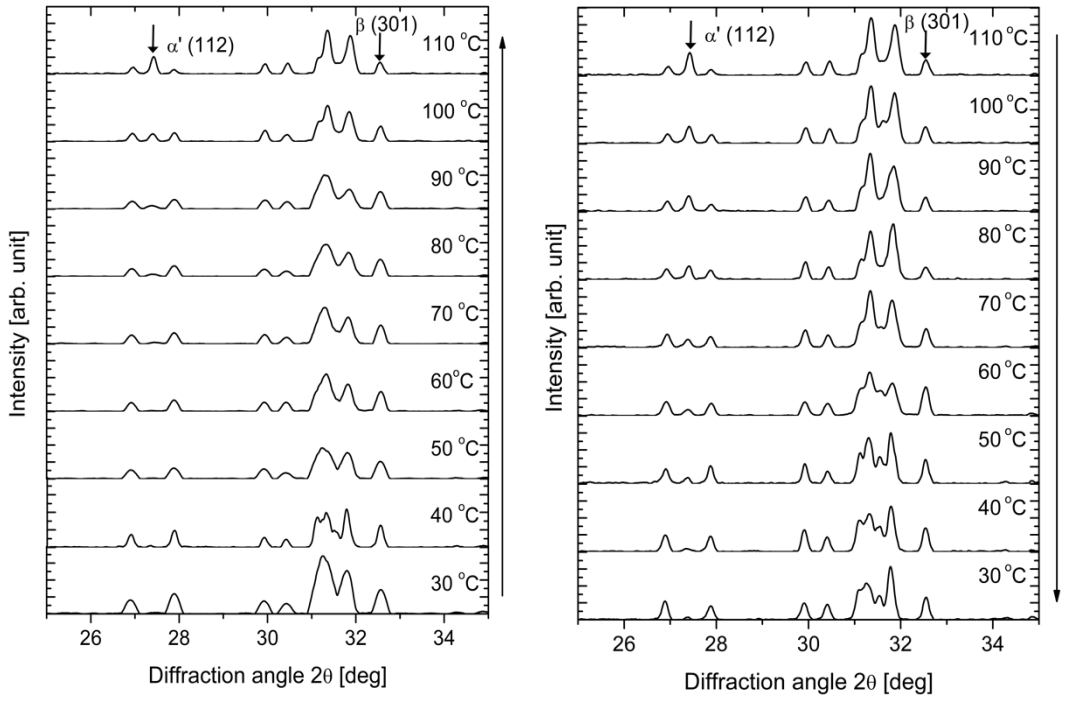


Fig. 3.3 XRD patterns of $Sr_2SiO_4:Eu^{2+}$ (3%) phosphors reduced at 1150 °C under $H_2/N_2$ ambient during (a) heating and (b) cooling process from 30 °C – 110 °C temperature range

The ratio of α' and β phase were estimated quantitatively as following method in order to clarify phase changes in the sample. Firstly, the XRD patterns of α' and β phases were simulated using ab initio structure determination, FOX [3.3] and crystal structure database, AtomWorks [3.4]. From the simulated patterns, the intensity of α' (112) and β (301) lines, lines, $I^o_{\alpha'}$ , $I^o_\beta$ were calculated. The volume ratio of β phase in the sample can be calculated as following equation.

$$r_\beta = \frac{I_\beta}{\left(\frac{I^o_\beta}{I^o_{\alpha'}}\right) I_{\alpha'} + I_\beta} \qquad (3.1)$$

where $I_{\beta}^{o}/I_{\alpha'}^{o}$ = 1.38, which is calculated by simulation. As shown in Fig. 3.4, the phase transition from β phase to α' phase can be observed over 80 °C during heating process, although there is small amount of β phase can observed at 110 °C. On the other hands, the phase transition from α' phase to β phase can be seen below 60 °C during cooling process. These results correspond to phase changes in XRD patterns in Fig. 3.3. Furthermore, the fitted lines explained well with the calculation and stimulation of β phase ratio in the samples.

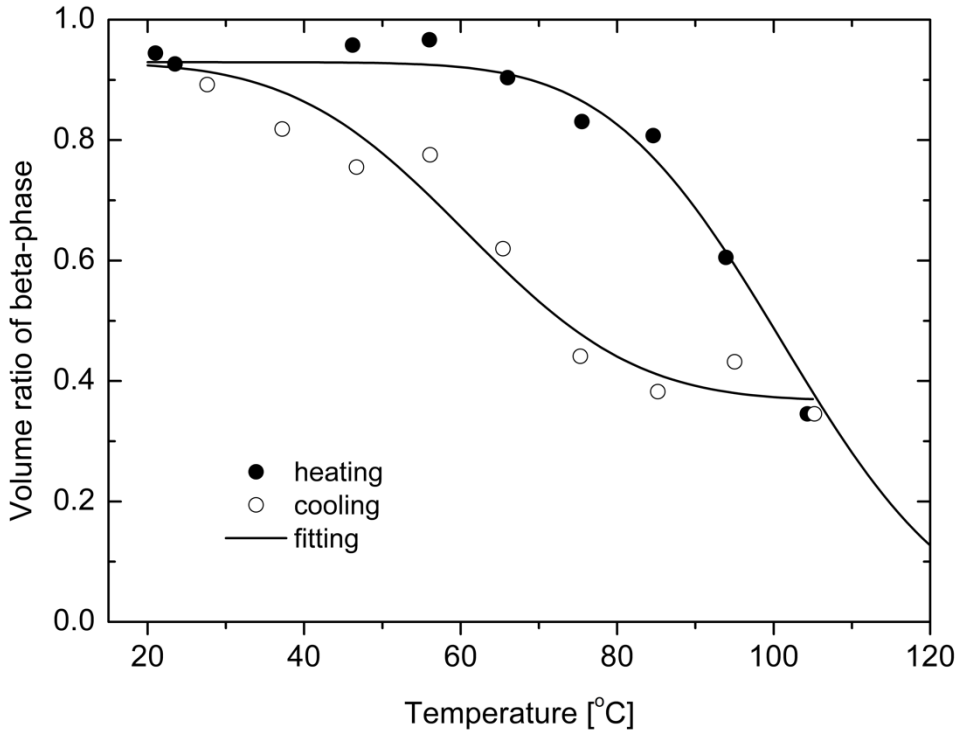


Fig. 3.4 Temperature dependence of β phase ratio of $Sr_2SiO_4:Eu^{2+}$ phosphors during heating and cooling process within 30 °C – 110 °C respectively

### 3.3.2 Temperature dependence of PL

On top of that, temperature dependence of PL spectra of $Sr_2SiO_4:Eu^{2+}$ phosphors also were investigated. The temperatures were set up from 30 °C to 200 °C for heating and vice versa for the cooling. At the beginning, the samples show emission band around 540 nm of β phase at 30 °C. As the temperature increases, PL intensity gradually decreases. Thermal quenching occurs and the emission band shifted to longer wavelength of α' phase can be observed around 80 °C. The emission bands of the samples show α' phase around 570 nm when the temperature up to at 200 °C. As the temperature decrease, PL intensity of the samples gradually increases and the emission bands shift from 570 nm of α' phase to 540 nm of β phase around 60 °C as shown in Fig. 3.5.

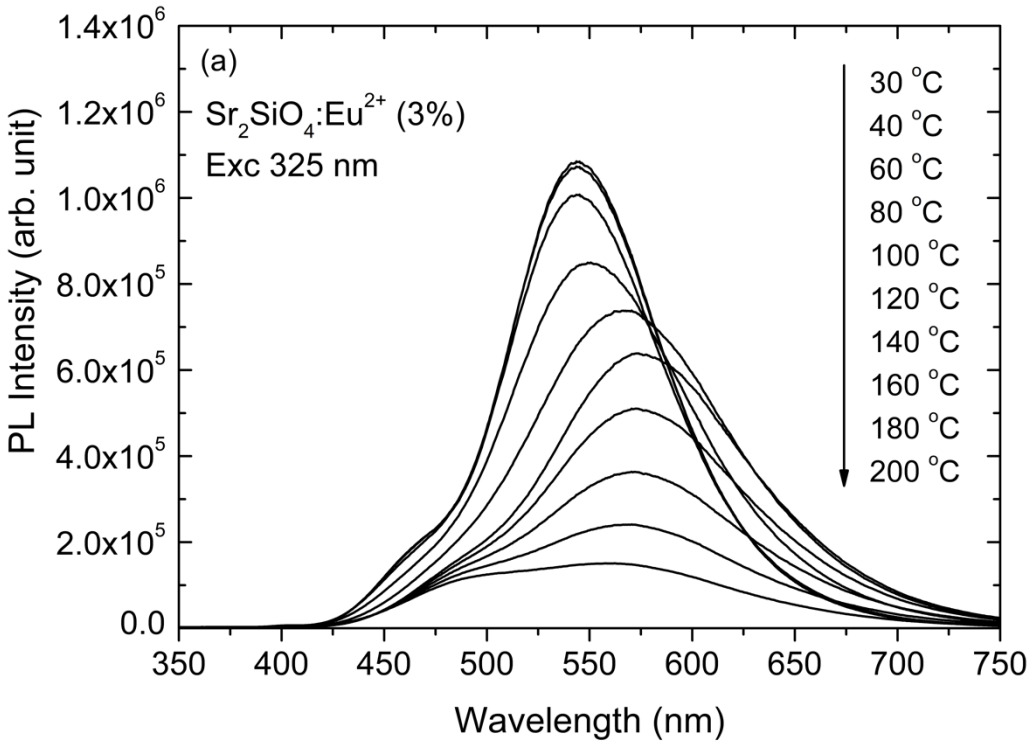

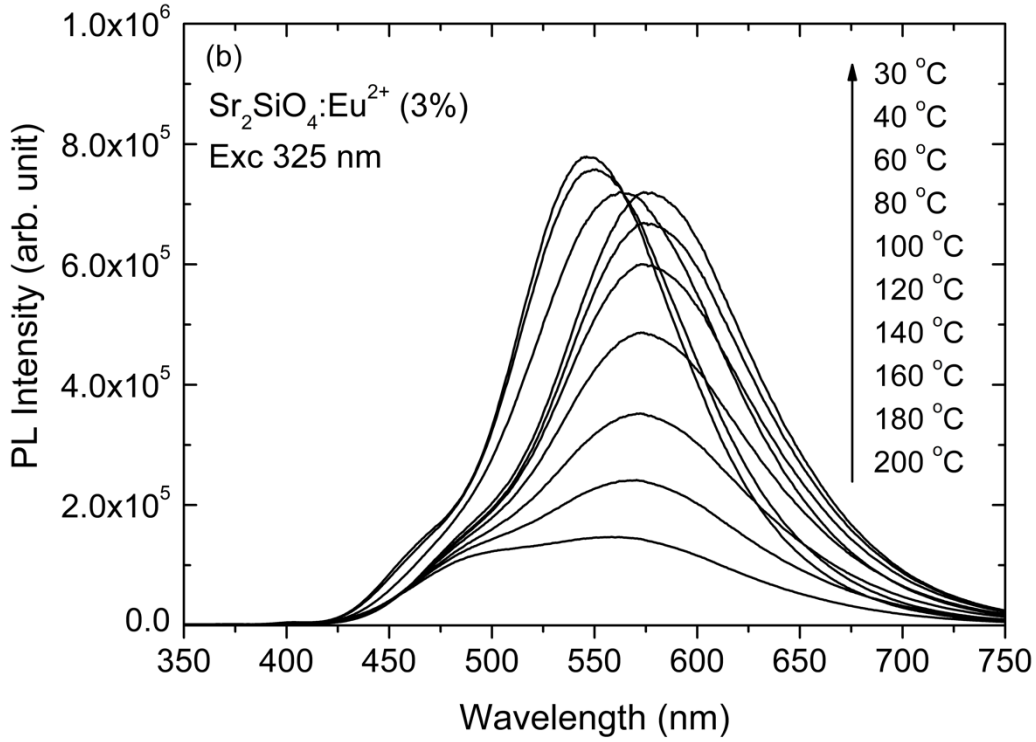


Fig. 3.5 PL spectra of $Sr_2SiO_4:Eu^{2+}$ (3%) phosphors reduced at 1150 °C under $H_2/N_2$ ambient during (a) heating and (b) cooling process in temperature range from 30 °C to 200 °C.

### 3.3.3 Analysis of $Sr_2SiO_4:Eu^{2+}$ (3%) phosphors hysteresis due to phase transition

The shift of emission bands was further analysed by decomposition into two Gaussian bands. In this study, we only used two bands for simply decomposition in order to investigate the phase transition of the samples. The center positions of the decomposed bands were calculated by least square fitting and the results are shown in Fig. 3.6. From the results, the center positions show that phase transition from β to α' phase occurs from 80 °C as the temperature increases. Meanwhile, phase transition from α' to β phase can be observed from 60 °C as temperature decreases. These results seem correspond to the XRD results in Fig. 3.4. Static hysteresis model of T. Barz et al. was applied [3.5] in order to evaluate the hysteresis behaviour observed in Fig. 3.4 and 3.6. This hysteresis model is heating rate independent and

the probability density function, $\phi_i$ of phase transition at temperature $T$ is assumed by following Gaussian distribution function with half maximum of $\sigma$,

$$\phi_i(T) = \frac{1}{\sqrt{2\pi}\sigma} e^{-\frac{(T-T_i)^2}{2\sigma^2}} \qquad (i = \text{heat, cool}) \tag{3.2}$$

where $T_i$ ($i$= heat, cool) are phase transition temperature during heating and cooling process. From eq. (3.2), the phase fraction is given using error function as follows,

$$\xi_i^0(T) = \int_{-\infty}^{T} \phi_i(\tau) d\tau = \frac{1}{2} + \frac{1}{2}\,\text{erf}\left(\frac{T-T_i}{\sqrt{2}\sigma}\right) \qquad (i = \text{heat, cool}) \tag{3.3}$$

where, $T_i$ is phase transition temperature during heating and cooling processes. $\xi_i^0(T)$ is the phase fraction when starting temperatures for heating and cooling are sufficiently lower or higher than phase transition temperature. The phase fraction $\xi_i(T)$ with specific starting temperature, $T_0$, for heating or cooling is given by following equations below.

$$\xi_{\text{heat}}(T) = 1 - \frac{1-\xi_{\text{heat}}(T_0)}{1-\xi_{\text{heat}}^0(T_0)} \cdot \left(1 - \xi_{\text{heat}}^0(T)\right) \tag{3.4a}$$

$$\xi_{\text{cool}}(T) = \frac{\xi_{\text{cool}}(T_0)}{\xi_{\text{cool}}^0(T_0)} \cdot \xi_{\text{cool}}^0(T) \tag{3.4b}$$

Phase ratio from XRD, $r_\beta$, in Fig. 3.4 is represented below by using eqs. (3.4a) and (3.4b),

$$r_{\alpha'} = 1 - r_\beta = (1 - k_{\alpha'})\xi_i(T) + k_{\alpha'} \qquad (i = \text{heat, cool}) \tag{3.5}$$

where, constant $k_{\alpha'}$ is the phase ratio of α' phase that remained after synthesis. The solid lines in Fig.18 show the fitted line using eq. (3.5). It is well explained to the experimental results with parameters, $T_{\mathrm{heat}}$ = 101℃, $T_{\mathrm{cool}}$ = 60.6℃, σ=17.3 K.

The shift of Eu emission bands in Fig. 3.6 will be affected by centroid shift, change in crystal field splitting [3.6] due to thermal expansion, and change in population distribution of excited states [3.7,3.8] as well as the phase transition. Here, assuming that higher order than second order can be omitted, center positions of Eu emission bands are represented by following equation.

$$E_{\mathrm{Eu}(1,2)} = \Delta E \cdot \xi_i(T) + aT^2 + bT + c \qquad (i = \mathrm{heat}, \mathrm{cool}) \tag{3.6}$$

The solid lines in Fig. 3.6 show the fitted line using eq. (3.6) and it is well explained with parameters, $T_{\mathrm{heat}}$ = 89.2℃, $T_{\mathrm{cool}}$ = 56.4℃, σ=9.20 K for Eu(1) and $T_{\mathrm{heat}}$ = 90.6℃, $T_{\mathrm{cool}}$ = 56.3℃, σ=18.3 K for Eu(2). It was found that there is about 40 K of thermal hysteresis, however there is 10 K of difference between the value of $T_{heat}$ in XRD and PL. The reason of the difference is not clear, but it is considered that the macroscopic structural change were observed in XRD, while change of the local environment surrounding Eu were observed in PL. Besides that, the difference between σ of Eu(1) and Eu(2) also exist and will be explained by the reason that phase fraction is not linear with center position, which should be estimated by intensity ratio of decomposed four PL bands in principle. The 40 K of thermal hysteresis observed for $Sr_2SiO_4$:$Eu^{2+}$ (3%) is much larger than undoped $Sr_2SiO_4$ of 10 K reported by M. Catti et al. [3.9]. This difference is to be related to the interference in the phase transition by Eu doping which discussed in chapter 2.

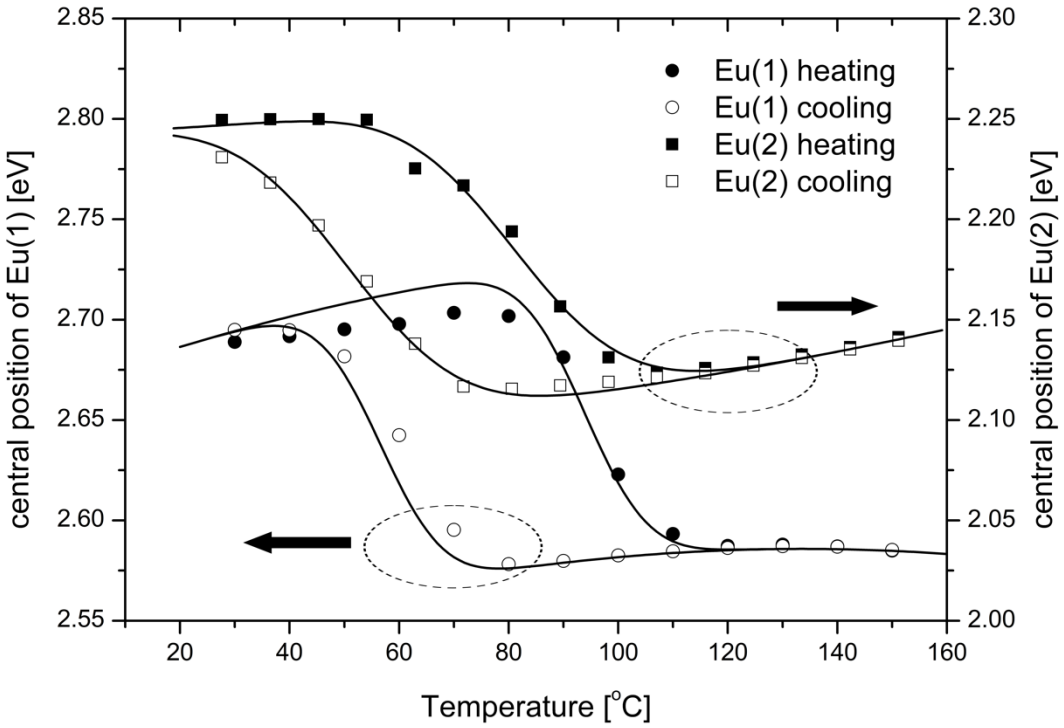


Fig. 3.6 Temperature dependence of central position od decomposed emission bands in PL spectra of $Sr_2SiO_4:Eu^{2+}$ (3%) phosphors during heating and cooling in temperature range from 30 °C – 150 °C.

## 3.4 Conclusion

In this study, the temperature dependence of crystal structure and PL spectra of $Sr_2SiO_4:Eu^{2+}$ (3%) phosphors were characterized to investigate the phase transition and thermal hysteresis between α' and β phase. Heating and cooling of the samples were done in temperature range from 30 °C–110 °C for XRD and 30 °C–200 °C for PL. Both XRD and PL results show that phase transition between β ↔ α' phase was observed around 80 °C during heating process and 60 °C during cooling process. The further analysis show that the thermal hysteresis between β ↔ α' directions of $Sr_2SiO_4:Eu^{2+}$ phosphors are about 40 K, which is much larger than the reported thermal hysteresis of undoped $Sr_2SiO_4$. Therefore, the appearance of phase transition in $Sr_2SiO_4:Eu^{2+}$ phosphors indicated that improved PCM was successfully demonstrated in silicate phosphors. As $Sr_2SiO_4:Eu^{2+}$ phosphors show green emission and have phase transition, it has adverse impact on the spectra distribution and light generated will unavoidably change by time as the operation of general white LEDs will easily surpass the transition point (85 °C). Therefore, Li introduction is the next step to fix the host lattice and tune to the suitable wavelength for high-power-white LEDs application.

## 3.5 References


[3.1] Zhen Song, Xianlin Ding, Shanshan Yang, Feifei Du, Liu Bian, Shanghong Duan, Q.L. Liu, Thermochromic material $Sr_2SiO_4:Eu^{2+}$ based on displacive transformation, J. Lumin. 152 (2014) 199–202.

[3.2] L.C. Ju, C. Cai, Q.Q. Zhu, J.Y. Tang, L.Y. Hao, X. Xu, Color tunable $Sr_2SiO_4:Eu^{2+}$ phosphors through the modification of crystal structure, J. Mater. Sci. Mater. Electron. 24 (2013) 4516–4521.

[3.3] V. Favre-Nicolin, R. Černý, FOX, "free objects for crystallography": A modular approach to ab initio structure determination from powder diffraction, J. Appl. Crystallogr. 35 (2002) 734–743.

[3.4] Y. Xu, M. Yamazaki, P. Villars, Inorganic materials database for exploring the nature of material, Jpn. J. Appl. Phys. 50 (2011) 1–5.

[3.5] T. Barz, A. Sommer, Modeling hysteresis in the phase transition of industrial-grade solid/liquid PCM for thermal energy storages, Int. J. Heat Mass Transf. 127 (2018) 701–713.

[3.6] P. Dorenbos, $Ce^{3+}$ 5d-centroid shift and vacuum referred 4f-electron binding energies of all lanthanide impurities in 150 different compounds, J. Lumin. 135 (2013) 93–104.

[3.7] P. Dorenbos, Energy of the first $4f_7$ - $4f_65d$ transition of $Eu^{2+}$ in inorganic compounds, J. Lumin. 104 (2003) 239–260.

[3.8] S.S.B. Nasir, A. Tanaka, S. Yoshiara, A. Kato, Luminescence properties of $Li_2SrSiO_4:Eu^{2+}$ silicate yellow phosphors with high thermal stability for high-power efficiency white LED application, J. Lumin. 207 (2019) 22–28.

[3.9] M. Catti, G. Gazzoni, The β ⇄ α' phase transition of $Sr_2SiO_4$. II. X-ray and optical study, and ferroelasticity of the β form, Acta Crystallogr. Sect. B. 39 (1983) 679–684.

# Chapter 4

# The preparation of $Li_2SrSiO_4:Eu^{2+}$ yellow silicate phosphors by improved PCM with different sintering temperature and Eu concentration

## 4.1 Introduction

From the previous chapter, $Sr_2SiO_4:Eu^{2+}$ phosphors were successfully synthesized by improved PCM using TEOS. It is known that $Sr_2SiO_4:Eu^{2+}$ phosphors have α' ↔ β phase transition when the temperature increases, where it is not really applicable in white LED application. Therefore, Li introduction were suggested to fix the phase transition in the host lattice and tune to suitable wavelength for white LEDs application.

In this study, the research about $Li_2SrSiO_4:Eu^{2+}$ phosphors were carried out. Among all the silicate phosphors, $Li_2SrSiO_4:Eu^{2+}$ phosphors possess blue excitation yellow phosphors, which have advantages in high luminescent properties, chemical and physical stability. With these advantages, it is possible to replace the conventional $YAG:Ce^{3+}$ in white LEDs application as $YAG:Ce^{3+}$ has low thermal stability. Although there are many research about the luminescent properties and thermal stability of the $Li_2SrSiO_4:Eu^{2+}$ phosphors, there is no detailed analysis and discussions about thermal stability of the phosphors [4.1,4.2]. In this chapter, $Li_2SrSiO_4:Eu^{2+}$ phosphors were synthesized by improved PCM using TEOS, which was successfully demonstrated in Chapter 2 and show good crystallinity properties. The sintering temperature dependence and Eu concentration dependence were investigated to find optimum synthesis condition for $Li_2SrSiO_4:Eu^{2+}$ phosphors.

## 4.2 Experimental procedures

$Li_2SrSiO_4:Eu^{2+}$ phosphors were synthesized by PCM using TEOS with different sintering temperature and Eu concentration (Eu = 0.25%, 0.5%, 0.75%. 1%, 3% and 5%). Fig. 4.1 show the synthesis flowchart of the samples. Firstly. The starting materials, $SrCO_3$ (kojundo, 99.9%), $LiCO_3$ (kojundo, 99.9%) and $Eu_2O_3$ (kojundo, 99.9%) were stoichiometrically weighted and dissolved in the mixture nitric acid and water at 100 °C. After the starting materials were completely dissolve in the solution, TEOS (nacalai, 95.0%), water and ethanol were added into the solution with the ratio of water : ethanol = 2:1. Ethanol are used in order to achieve smooth reaction between TEOS and water as TEOS is water insoluble, which reported by X.Y. Tzai [4.3]. Then, citric acid monohydrate (nacalai, 99.0%) as chelating agent was added and strirred at 80 ºC for 12 hours above. After all the materials were chelated for 12 hours, propylene glycole was added for gelation process at 100 ºC for 3 hours. Next, obtained gel was heated for 3 hours at 350 º C to remove theorganic materials and the precursors can be obtained. After pyrolysis at 350 ºC, the precursor were put into an alumina boat and calcined in air at 700 ºC by electric furnace for another 3 hours. Lastly, the precursors were sintered at temperature range of 700 ºC – 900 ºC of temperature range for 6 hours under $H_2/N_2$ (5% $H_2$/95% $N_2$) reduction atmosphere to obtain $Li_2SrSiO_4:Eu^{2+}$ phosphors.

$Li_2SrSiO_4:Eu^{2+}$ (1%) phosphors were also synthesized by SSR for comparison. Firstly, the staring materials $SrCO_3$ (kojundo, 99.9%), $LiCO_3$ (kojundo, 99.9%), $Eu_2O_3$ (kojundo, 99.9%) and $SiO_2$ (99.9%, nacalai) were weight stoichiometrically and all the starting materials were mixed and grind together for 1 hour. After 1 hour, the mixed and ground materials were calcined at 600 ºC for 3 hours by air using electrical furnace to obtain white precursor. Lastly, the white precursors were sintered at 900 ºC for 6 hours under $H_2/N_2$ ambient. The evaluation of XRD and PL are similar in Chapter 2 (section 2.2). The morphology of the samples were

identified by the field emission scanning electron microscopic (FE-SEM, Hitachi S-4000) with 15 kV of accelerate voltage.

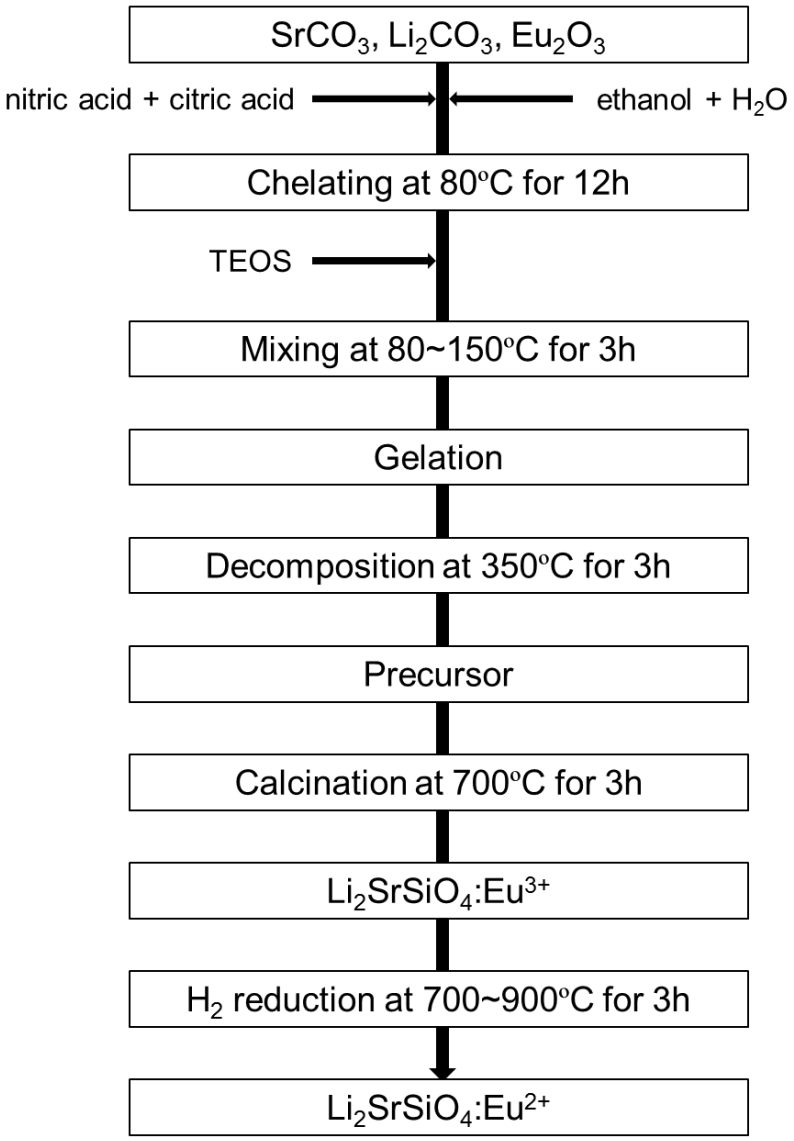


Fig. 4.1 Synthesis flowchart of $Li_2SrSiO_4:Eu^{2+}$ phosphors by improved PCM

## 4.3 Results and discussions

### 4.3.1 Sintering temperature dependence

The crystal structure of $Li_2SrSiO_4:Eu^{2+}$ (1%) phosphors prepared with different sintering temperature were investigated by XRD diffraction as shown in Fig. 4.2. The sintering temperature range is from 700 °C to 900 °C. The crystal structure of $Li_2SrSiO_4:Eu^{2+}$ (1%) phosphors prepared at 900 °C by SSR also were shown for comparison. From Fig. 5.2, all the samples $Li_2SrSiO_4:Eu^{2+}$ phosphors prepared either PCM or SSR lines match with ICDD data of $Li_2SrSiO_4$. Moreover, there are no secondary phases can be observed for all the samples. These XRD results indicate that $Li_2SrSiO_4:Eu^{2+}$ phosphors were successfully synthesized at lower temperature with high crystallinity by using PCM compared SSR, which high temperature is required. The temperature limit for the samples is 900 °C due to the samples melts above 950 °C.

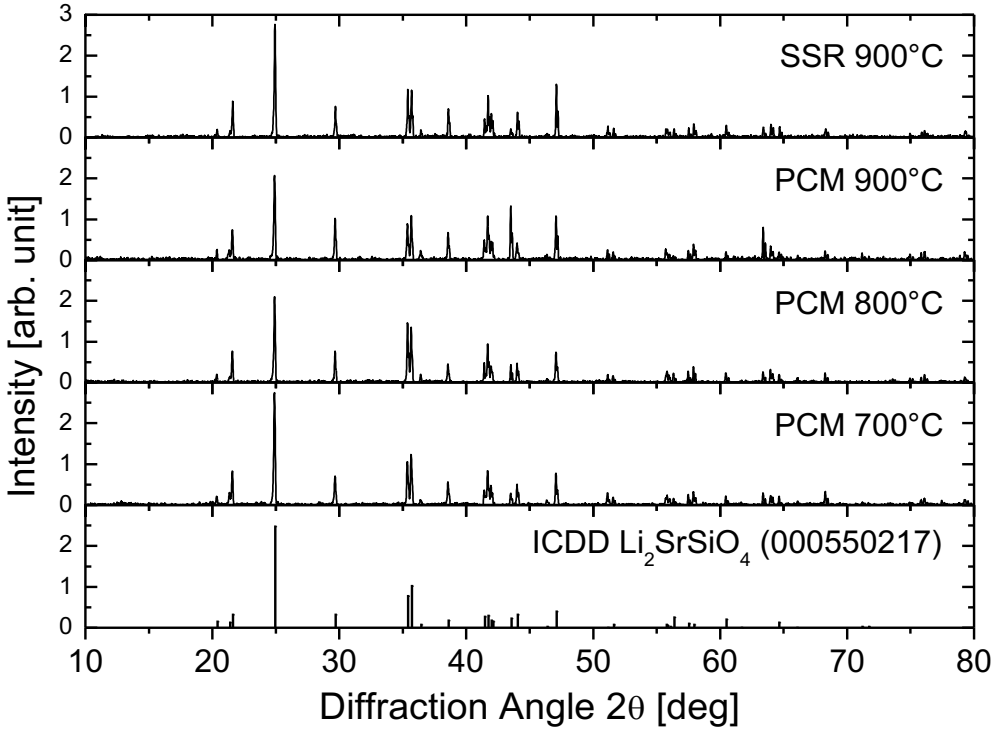


Fig. 4.2 XRD patterns of $Li_2SrSiO_4:Eu^{2+}$ (1%) phosphors with different reduction temperatures

The surface morphology of $Li_2SrSiO_4:Eu^{2+}$ (1%) phosphors with different sintering temperature were also identified by SEM images as shown in Fig. 4.3. Although there are no significant changes in XRD patterns, the morphological results reveal observable changes in particles size. As shown in Fig. 4.3, the samples with 700 °C reduction temperature show the small particles size within 3 – 5 µm. When the temperature increases to 800 °C and 900 °C, the particles size was getting bigger within 4 – 8 µm and 13 -15 µm respectively. The samples prepared at 900 °C by SSR show the biggest particles size compared to PCM within 30 µm. The samples prepared by PCM shows smaller particles size compared to SSR. Indicating that the homogenous composition of the samples can be synthesized through improved PCM.

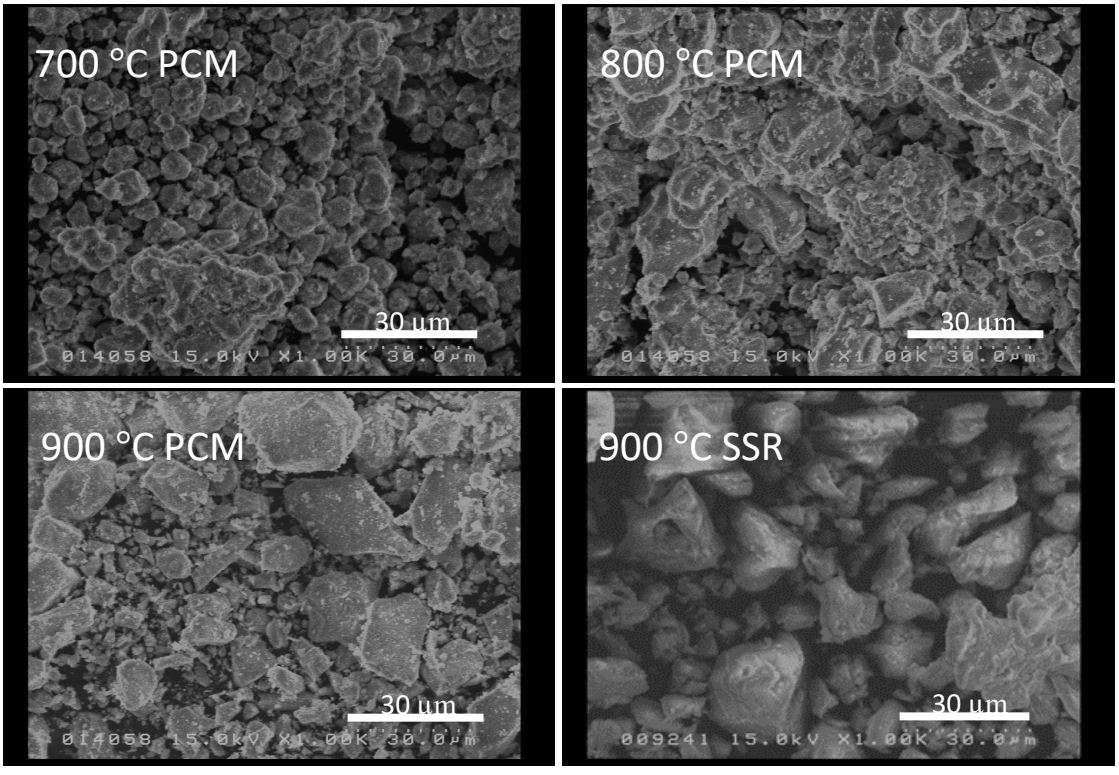


Fig. 4.3 SEM images of $Li_2SrSiO_4:Eu^{2+}$ (1%) phosphors with different reduction temperatures prepared by PCM and SSR at 900 ºC reduction temperature for comparison.

The PL spectra of $Li_2SrSiO_4:Eu^{2+}$ (1%) phosphors with different sintering temperature by both PCM and SSR were investigated. As shown in Fig. 4.4, all the samples exhibit broad yellow emission band around 580 nm under 325 m excitation light, which is same with previous reports [4.4–4.6]. PL intensity of the samples prepared by PCM increases as sintering temperature increases. This is due to good crystallinity when the temperature increases, resulting in high PL intensity for the samples were synthesized by PCM. The samples prepared at 900 °C shows the highest PL intensity. Meanwhile, the samples were prepared by SSR show the lowest PL intensity although the samples sintered at highest sintering temperature same with PCM (900 °C). Moreover, the result reveals that the PL intensity of samples synthesized by PCM show 7 times higher than SSR. As the samples will melt at 950 °C, the limit of sintering temperature is set until 900 °C. For the Eu concentration dependence in next section, 900 °C sintering temperature is used for the synthesis of the sample.

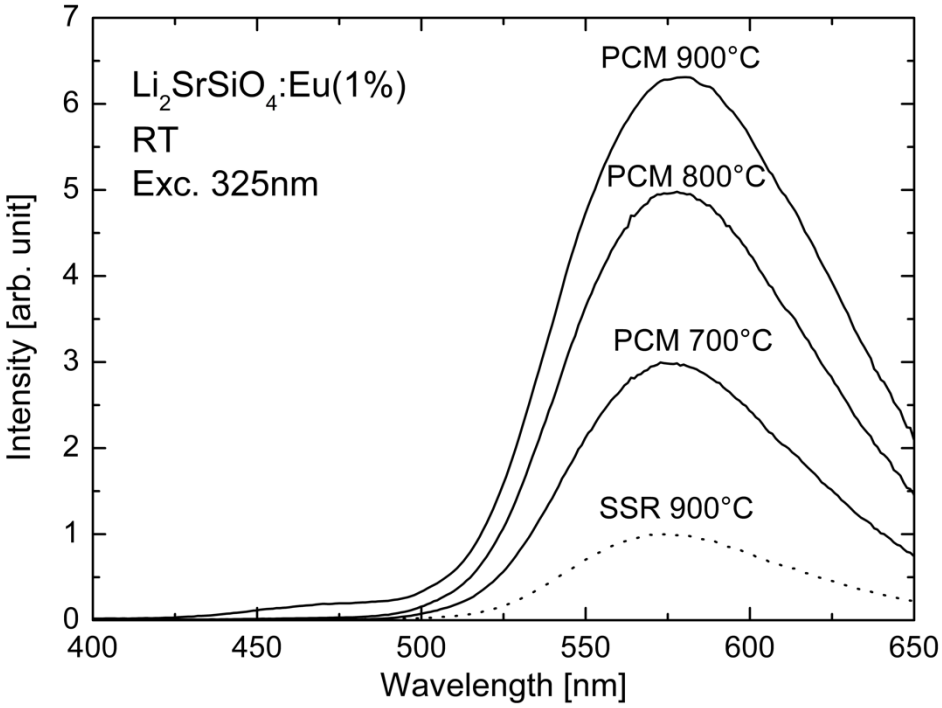


Fig. 4.4 PL spectra of $Li_2SrSiO_4:Eu^{2+}$ (1%) phosphors with different reduction temperature measured in room temperature. Dotted line represents the PL spectra of $Li_2SrSiO_4:Eu^{2+}$ (1.0%) phosphor prepared by SSR.

### 4.3.2 Eu concentration dependence

From the previous section, $Li_2SrSiO_4:Eu^{2+}$ (1%) phosphors at 900 °C shows the highest PL intensity. Therefore, in this section, $Li_2SrSiO_4:Eu^{2+}$ phosphors were synthesized at 900 °C by PCM with different Eu concentration to investigate the Eu concentration dependence. Eu concentration was set from 0.25%, 0.5%, 0.75%, 1%, 3% and 5%. The crsytal structure of the $Li_2SrSiO_4:Eu^{2+}$ phosphors were synthesized at 900 °C by PCM with different Eu concentration is shown in Fig. 4.5. All the samples show identical XRD lines from ICDD data $Li_2SrSiO_4$ and there no secondary phases can be observed. The samples with 0.5% Eu concentration show the strongest peak intensity around 25 ° among all the samples.

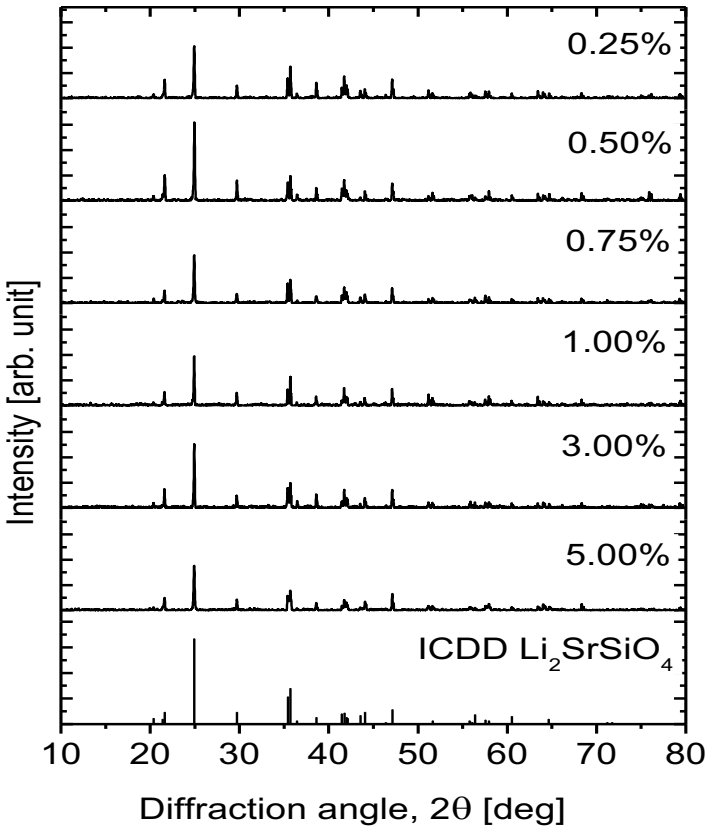


Fig. 4.5 XRD patterns of $Li_2SrSiO_4:Eu^{2+}$ phosphors with different Eu concentrations at 900 ºC reduction temperature

PL spectra of $Li_2SrSiO_4:Eu^{2+}$ phosphors sintered at 900 °C with different Eu concentrations were investigated. From Fig. 4.6, all the samples show broad yellow emission band around 570 nm and $Li_2SrSiO_4:Eu^{2+}$ (0.5 %) phosphors show the highest PL intensity among other Eu concentration. Concentration quenching occurred at 0.75% Eu concentration above. PL intensity decreases as Eu concetration increases due to the energy transfer between $Eu^{2+}$ in different sites of the host lattice and cause to concentration quenching [4.7]. From the XRD results, there are no secondary phase such as β-$Sr_2SiO_4:Eu^{2+}$ can be observed. However, PL results shows clearly a weak blue emission from β-$Sr_2SiO_4:Eu^{2+}$ can be observed, which is due to loss of Li atoms at high temperature. In addition, emission of β-$Sr_2SiO_4:Eu^{2+}$ can also be observed in low Eu concentration at 474 nm and 535 nm, while the PLE peaks are at 325 nm and 375 nm was reported by Guo et al.[4.8].

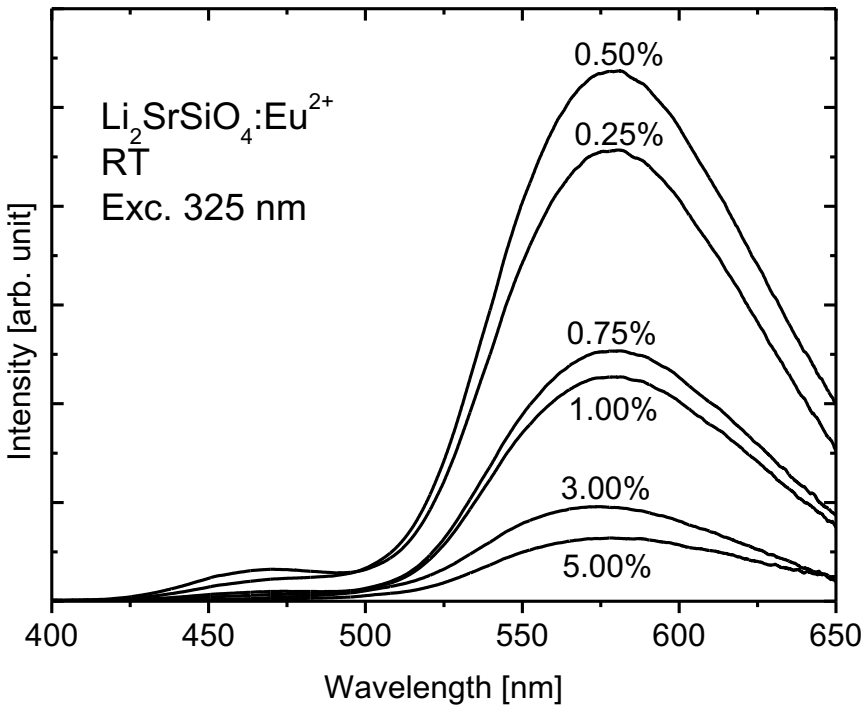


Fig. 4.6 PL spectra of $Li_2SrSiO_4:Eu^{2+}$ phosphors with different Eu concentration measured at room temperature.

### 4.3.3 Eu concentration quenching

Eu concentrated dependence of integrated PL intensity of $Li_2SrSiO_4:Eu^{2+}$ phosphors were investigated (Fig. 4.7). From Fig. 4.7, the optimum Eu concentration for the $Li_2SrSiO_4:Eu^{2+}$ phosphors is 0.5% and concentration quenching can be observed above 0.5%. Dexter theory [4.9] stated that the types of interaction which control the concentration quenching can be determined from the change in emission intensity of the activator by the variation of average distance between activators; i.e. activator concentrations. The emission intensity (I) per activators ion follows the Eq. (4.1) [4.7,4.9,4.10] stated below.

$$\frac{I}{x} = K\left(1 + \beta x^{\frac{Q}{3}}\right)^{-1}, \qquad (4.1)$$

where $x$ is activator concentration, $K$ and $\beta$ are constant for the same excitation conditions for the samples. The value of $Q$ represents the types of multipolar interaction between activators.

$Q = 6$ , dipole-dipole (d-d)

$Q = 8$ , dipole-quadrupole (d-q)

$Q = 10$ , quadrupole - quadrupole (q-q)

From Fig. 4.7, the inset shows the graph of $I/x$ vs. $x$ in log scale and fitted line by Dexter's theory with values of $Q$ is 5.75. The values of $Q$ relatively near to $Q = 6$; which determined that d-d interactions are resulting in the quenching concentration. The fitted line well-explained with observed PL intensity in Fig. 4.7. Therefore, $Li_2SrSiO_4:Eu^{2+}$ phosphors prepared by PCM lead to the uniform distribution of Eu in the phosphors, resulting to an excellent luminescent properties.

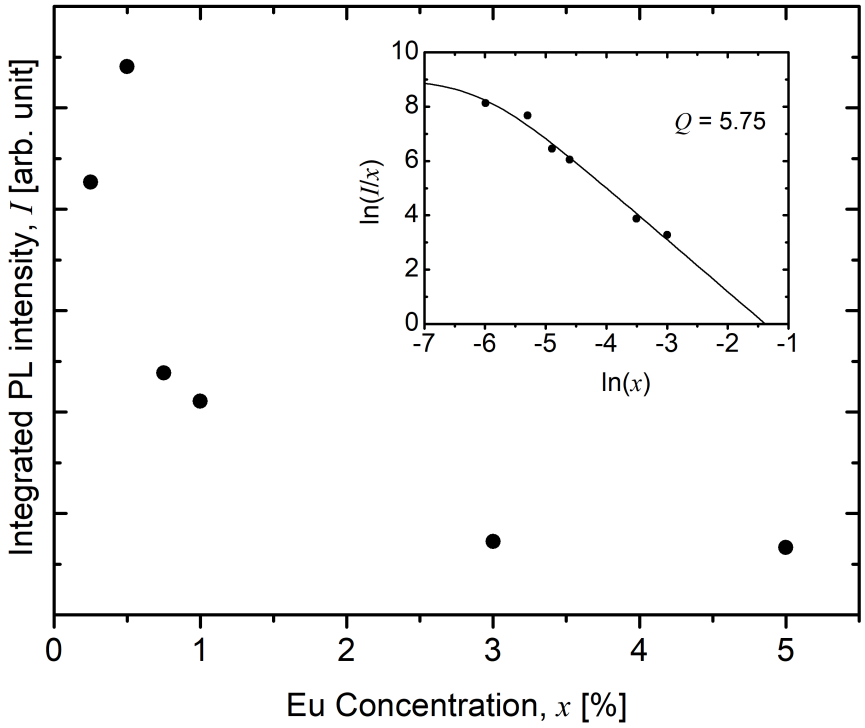


Fig. 4.7 Eu concentration dependence of integrated PL intensity of $Li_2SrSiO_4:Eu^{2+}$ phosphors. Closed circles show the PL intensity of the samples and solid line in inset represents fitted line by Dexter's theory

## 4.4 Conclusion

In this study, sintering temperature dependence and Eu concentration of $Li_2SrSiO_4:Eu^{2+}$ phosphors were investigated. Firstly, $Li_2SrSiO_4:Eu^{2+}$ (1%) phosphors were synthesized by PCM with sintering temperature range from 700 °C – 900 °C. $Li_2SrSiO_4:Eu^{2+}$ (1%) phosphors were also synthesized by SSR at 900 °C for comparison. The XRD results show all the samples prepared either PCM or SSR show identical XRD peaks from ICDD data and there are no secondary phases can be observed. Besides that, $Li_2SrSiO_4:Eu^{2+}$ (1%) phosphors were successfully synthesized at low temperature (700 °C) by improved PCM compared to SSR, which high temperature is required. It indicates that homogenous solution can be synthesized, which leading to good crystallinity through improved PCM. On top of that, SEM images shows that the particle sizes of the samples with 700 °C, 800 °C and 900 °C prepared by improved PCM are within 3 - 5 μm, 4 - 8 μm and 13-15 μm respectively, which indicating that the particles size of the samples increases as sintering temperature increases. The samples were prepared by SSR at 900 °C show the biggest particle size within 30 μm. For the PL spectra, all the samples show yellow emission band around 570 nm. PL intensity of the samples prepared by PCM increases as temperature increases. The samples at 900 °C by PCM show the highest PL intensity among all the samples. Meanwhile, the samples at 900 °C by SSR show the lowest PL intensity.

For Eu concentration, $Li_2SrSiO_4:Eu^{2+}$ phosphors were synthesized by improved PCM with different Eu concentration (0.25%, 0.5%, 0.75%, 1%, 3% and 5%). The XRD patterns show that all the samples show identical XRD peaks and also no secondary peaks can be observed. $Li_2SrSiO_4:Eu^{2+}$ (0.5%) phosphors show the strongest XRD peaks around 27 °. Besides that, PL spectra of all the samples show a broad yellow emission band around 570 nm and $Li_2SrSiO_4:Eu^{2+}$ (0.5%) phosphors shows the highest PL intensity. The PL intensity of the samples decreases as Eu concentration increase, which leading to concentration quenching.

The concentration quenching occurred at 0.75% Eu concentration above. However, weak blue emission from β-$Sr_2SiO_4$:$Eu^{2+}$ can be observed although there is no β-$Sr_2SiO_4$ peaks appeared in XRD results. Eu concentration quenching is well explained by Dexter's theory and dominated by dipole-dipole interaction between Eu ions. From the results above, improved PCM using TEOS were successfully demostrated in the synthesis of $Li_2SrSiO_4$:$Eu^{2+}$ phosphors, which show higher emission intensity and can be synthesized at lower temperature compared to SSR. Therefore, the thermal stability of $Li_2SrSiO_4$:$Eu^{2+}$ (0.5%) sintered at 900 °C will be further investigated in the next chapter.

## 4.5 References


[4.1] V.P. Dotsenko, S.M. Levshov, I.V. Berezovskaya, G.B. Stryganyuk, A.S. Voloshinovskii, N.P. Efryushina, Luminescent properties of Eu2+ and Ce3+ ions in strontium litho-silicate $Li_2SrSiO_4$, J. Lumin. 131 (2011) 310–315.

[4.2] Pan Li You, Study on the Morphology and Thermal Stability of $Li_2SrSiO_4:Tb^{3+}$ Materials, Adv. Mater. Res. 989–994 (2014) 437–440.

[4.3] S.D. Wang, X. Tzai, Effects of adding different proportions of ethanol or water / ethanol on performance of hydrophobic antireflection film, Surf. Eng. 27 (2011) 272–278.

[4.4] S.M. Levshov, I. V Berezovskaya, N.P. Efryushina, B.I. Zadneprovskii, V.P. Dotsenko, Synthesis and Luminescence Properties of $Eu^{2+}$-Doped $Li_2SrSiO_4$, Inorg. Mater. 47 (2011) 285–289.

[4.5] H. He, R. Fu, H. Wang, X. Song, Z. Pan, X. Zhao, X. Zhang, Y. Cao, $Li_2SrSiO_4:Eu^{2+}$ phosphor prepared by the Pechini method and its application in white light emitting diode, J. Mater. Res. 12 (2008) 36–39.

[4.6] R.D. Shannon, Revised Effective Ionic Radii and Systematic Studies of Interatomie Distances in Halides and Chaleogenides Central Research and Development Department , Experimental Station , E . L Du Pont de Nemours The effective ionic radii of Shannon & Prewitt, Acta, Acta Crystallogr. Sect. A. 32 (1976) 751–767.

[4.7] G. Blasse, B.C. Grabmaier, Luminescent Materials, Springer-Verlag, Berlin Heidelberg New York, 1994.

[4.8] C. Guo, Y. Xu, F. Lv, X. Ding, Luminescent properties of $Sr_2SiO_4:Eu^{2+}$ nanorods for near-UV white LED, J. Alloys Compd. 497 (2010) L21–L24.

[4.9] D.L. Dexter, A Theory of Sensitized Luminescence in Solids, J. Chem. Phys. 21 (1953) 836–850.

[4.10] L.G. Van Uitert, Characterization of Energy Transfer Interactions between Rare Earth Ions, J. Electrochem. Soc. 114 (1967) 1048–1053.

# Chapter 5

# Thermal stability and quenching of $Li_2SrSiO_4:Eu^{2+}$ yellow silicate phosphors

## 5.1 Introduction

Temperature quenching and thermal stability of phosphors are important factors for the white LED application. Generally, when the white LEDs are operating for long periods, the temperature within phosphors and white LEDs increases. When the temperature achieve at 150 °C above, it will lead to the phosphor deterioration in white LEDs and damage out the phosphors [5.1,5.2]. High temperature will lead to decrease in emission intensity and change in emission color phosphors. As a result, it will affect the efficiency and colour chromaticity of white LEDs. In order to solve these problems, high thermal stability of phosphors are needed for long term used in white LEDs.

There are many reports regarding thermal stability of YAG:$Ce^{3+}$ [5.3–5.6]. However, low thermal stability is the major problems of this phosphors. On top that, there are also many reports about $Li_2SrSiO_4:Eu^{2+}$ phosphors in the aspect of optical properties, crystal structure and some of them also reported about temperature dependence, which related to thermal stability [5.7–5.22]. However, there is no detailed analysis and discussion to prove that $Li_2SrSiO_4:Eu^{2+}$ yellow phosphors have high thermal stability, which can be feasible replacement of YAG:$Ce^{3+}$ phosphors. In this chapter, PL spectra of $Li_2SrSiO_4:Eu^{2+}$ (0.5%) yellow phosphors, which were synthesized by improved PCM, were measured from low to high temperature to investigate the thermal stability of the samples.

## 5.2 Experimental

Thermal stability of the $Li_2SrSiO_4:Eu^{2+}$ phosphors were investigated by PL spectra of the samples at low and high temperature ranges from 16 K – 300 K (room temperature) and 300 K – 483 K. The samples were cooled by cryostat equipped with cooling refrigerator (Iwatani Cryo-Mini D105) to measure the PL spectra at low temperature. For PL spectra at high temperature, soldering iron, single phase power regulator and programmable temperature controller were set up, which are similar in Chapter 3 (section 3.2).

## 5.3 Results and discussion

### 5.3.1 Temperature dependence

The thermal quenching of the phosphors is affected by host lattice vibration. In order to investigate the original emission from the phosphors, the PL spectra of the samples were measured at low temperature, which can limit the lattice vibration in the samples. Therefore, PL and PLE spectra of the $Li_2SrSiO_4:Eu^{2+}$ (0.5%) phosphors at l6.5 K were measured, where the excitation and monitoring wavelength for PL and PLE spectra are 325 nm and 560 nm respectively. From Fig. 5.1, the peak energy of PL band is 2.1 eV, while main PLE bands are situated between 2.7 – 3.7 eV. The obtained PL and PLE spectra reveal that $Li_2SrSiO_4:Eu^{2+}$ (0.5%) phosphors can be promising yellow phosphors for the combination with blue chips LED for the fabrication of white LEDs.

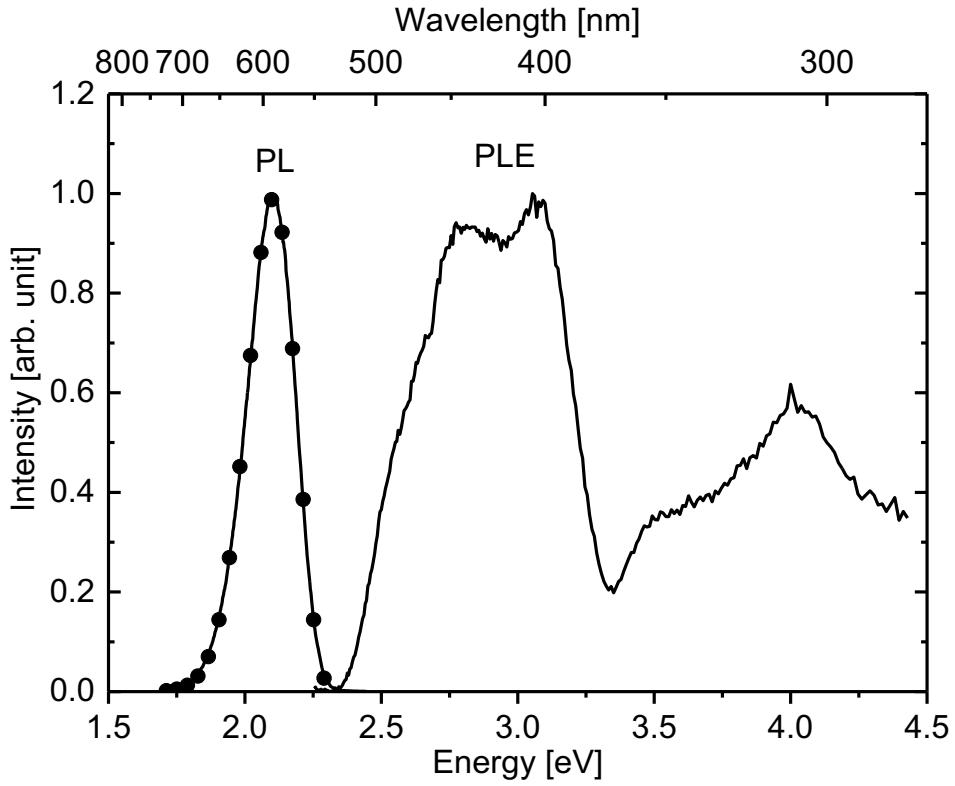


Fig. 5.1 PL and PLE spectra of $Li_2SrSiO_4:Eu^{2+}$ (0.5%) phosphor at 16.5 K. The excitation and monitoring wavelength for PL and PLE spectra are 325 nm 580 nm respectively. Closed circles represent the Poisson distribution and is fitted for the PL spectra

In order to investigate the thermal stability of the phosphors, PL spectra measurement of $Li_2SrSiO_4:Eu^{2+}$ (0.5%) phosphors at low and high temperature were carried out at the temperature range from 16.4 K to 300 K (room temperature) and 300 K to 483 K as shown in Fig. 5.1. From the PL results, all the samples exhibit yellow broad emission band around 560 nm. It can be observed that the PL intensity decreases as temperature increases, which indicating thermal quenching of the samples. Moreover, the shift of emission bands to higher energy sides can be observed as increasing in temperature, which due to following reasons.

(1) reduction of crystal field due to increase of the lattice constant of the samples with thermal expansion. The energy level of the lowest excited state of 5d levels becomes higher with the reduction of crystal field.

(2) the occupation of higher vibronic levels of the lowest excited state of 5d levels by thermal excitation. The PL band is shifted and broaden to high energy region with the increase of the emission from higher vibronic levels.

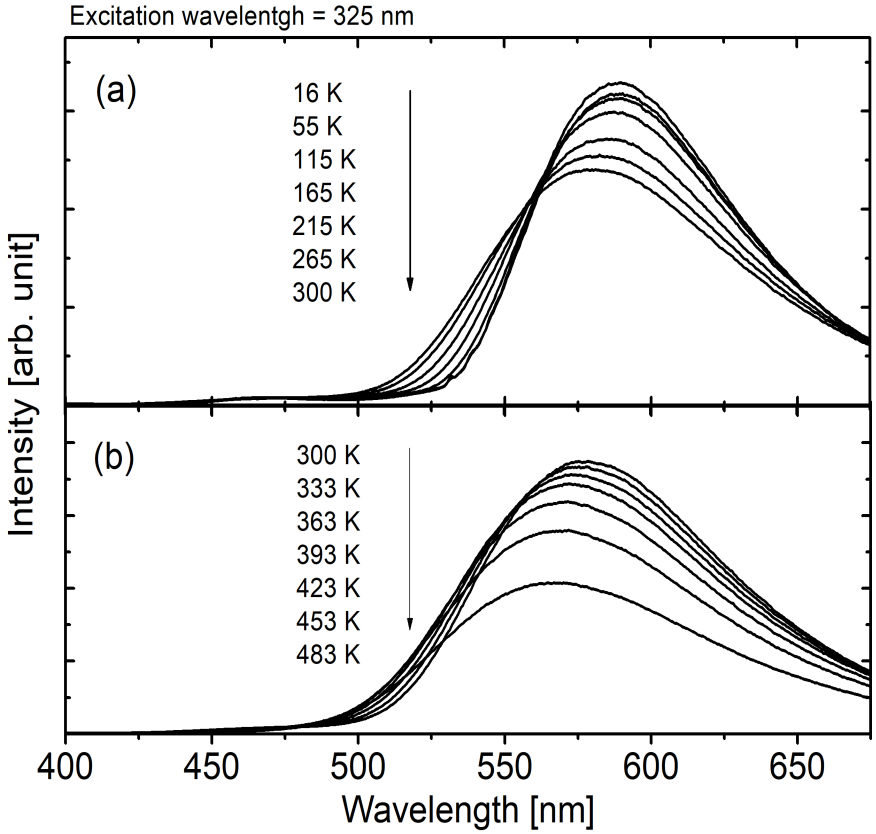


Fig. 5.2 PL spectra of $Li_2SrSiO_4:Eu^{2+}$ (0.5%) measured at temperature range (a) 16 K – 300 K and (b) 300 K – 483 K

### 5.3.2 Spectral shape of PL band in low temperature range

$Eu^{2+}$ emission at low temperature shown in Fig. 5.1 was fitted by the Poisson distribution [5.23].

$$f(E) \propto \frac{S^{\frac{|E_0-E|}{\hbar\omega}} e^{-S}}{\left(\frac{|E_0-E|}{\hbar\omega}\right)!}, \qquad (5.2)$$

where $E_0$, $S$ and $\hbar\omega$ represent zero phonon energy, Huang-Rhys factor and energy of phonon coupled with the emission at ground state respectively. Each of fitting parameter for PL spectra was concluded in Table.5, based on the calculation using eq. (5.2). The fitting results were well presented with the PL spectrum of the samples as shown in Fig. 5.3. Meanwhile, PLE spectra of $Li_2SrSiO_4:Eu^{2+}$ (0.5%) phosphors in Fig. 5.3 shows the complicated excitation band structures due to intra 4f-5d Eu transition, transition from Eu to the conduction band and others, which difficulty in fitting. The emission of $Li_2SrSiO_4:Eu^{2+}$ (0.5%) phosphors indicate the phonon terminated emission and the phonon energy is 38.5 meV.

Table. 5.1 Fitting parameters for PL bands in low temperature by Poisson distribution

| | $E_0$ [eV] | $S$ | $\hbar\omega$ [meV] |
|---|---|---|---|
| PL | 2.29 | 5.36 | 38.5 |

Fig. 5.3 shows full width half maximum (FWHM) of $Li_2SrSiO_4:Eu^{2+}$ (0.5%) phosphors at temperature range from 16.4 K to 300 K. Generally, Temperature dependence of FWHM of PL band follows the Eq. (5.3) below [5.24], Reshchikov et al., assumes that ground state and excited state of phonon energy are same [5.24]. From this assumption, 0.38 eV of phonon energy at ground state estimated from eq. (5.2) is used in following eq. (5.3),

$$W(T) = W(0)\sqrt{\coth\frac{\hbar\omega}{2kT}}\,. \qquad (5.3)$$

where $W(T)$ represents FWHM of emission band at temperature $T$, $k$ is Boltzmann constant, and $\hbar\omega$ is energy of phonon coupled with emission at excited state. In Fig. 5.3, the measured FWHM of the $Li_2SrSiO_4:Eu^{2+}$ (0.5%) phosphors from 16.4 K to 300 K were well-explained by using 0.38 eV (solid line in Fig. 5.3). Peak energy of PLE band $E_{PLE}$, that of PL band $E_{PL}$ and Stokes shift $\Delta E$ can be calculated using the same phonon energy by following equations (5.4a - 5.4c),

$$E_{PLE} = E_0 + \left(S - \frac{1}{2}\right)\hbar\omega\,, \qquad (5.4a)$$

$$E_{PL} = E_0 - \left(S - \frac{1}{2}\right)\hbar\omega\,, \qquad (5.4b)$$

$$\Delta E = E_{PLE} - E_{PL} = (2S - 1)\hbar\omega\,, \qquad (5.4c)$$

and estimated to be 2.48 eV, 2.10 eV and 0.38 eV respectively. The estimated $E_{PL}$ coincides with the peak energy of PL band and $E_{PLE}$ probably correspond with the slight shoulder in lower energy side of main PLE band in Fig. 5.1. $E_{PLE}$ is in blue region. Therefore, the $Li_2SrSiO_4:Eu^{2+}$ phosphors can be one of the promising yellow emission with the blue excitation phosphor for white LEDs application.

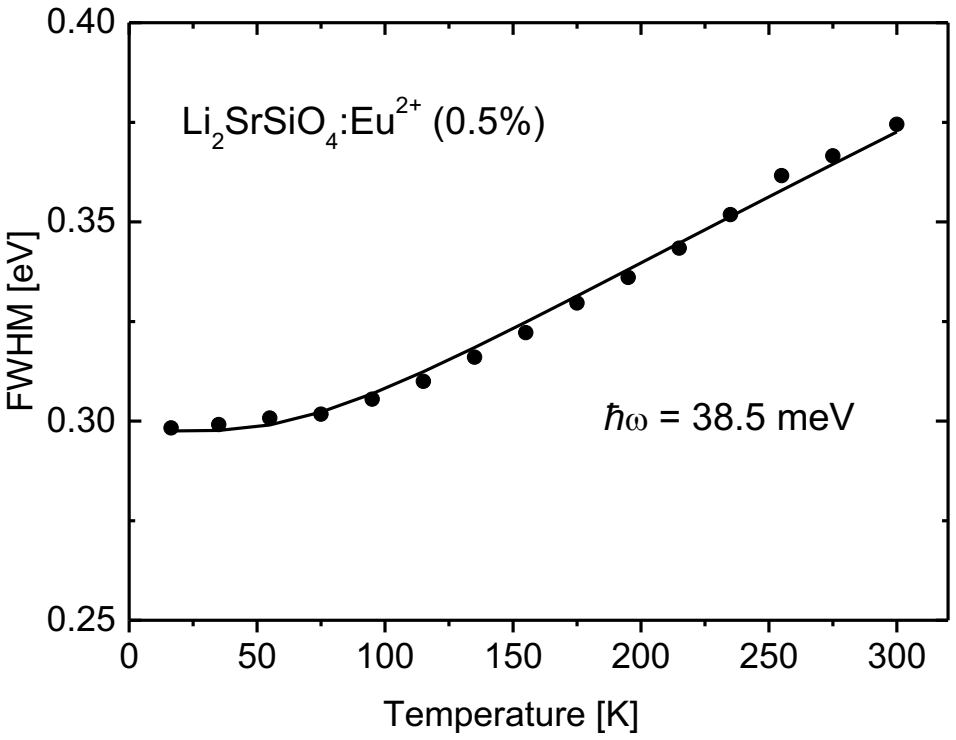


Fig. 5.3 Temperature dependence of FWHM of PL band of $Li_2SrSiO_4:Eu^{2+}$ (0.5%). Solid line represents fitted line based on eq. (5.3)

### 5.3.3 Temperature quenching

As the white LEDs will damage out when the temperatures reach to 150 °C (423 K), high thermal stability of phosphors are required for white LEDs application. In order to investigate the thermal stability, the temperature range was set up from 300 K to 480 K and temperature dependence of integrated PL intensity of $Li_2SrSiO_4:Eu^{2+}$ (0.5%) phosphors were investigated as shown in Fig. 5.4. The results reveal that the PL intensity of the sample is about 80% at 423 K, which indicates that $Li_2SrSiO_4:Eu^{2+}$ (0.5%) phosphors have high temperature stability compared to $YAG:Ce^{3+}$ phosphors [5.4]. Temperature dependence of PL intensity due to temperature quenching were fitted by the following Arrhenius equation [5.25],

$$I(T) = I(0)\left(1 + se^{-\frac{\Delta E}{kT}}\right)^{-1}. \quad (5.5)$$

where, $\Delta E$ is activation energy of temperature quenching process, $s$ is frequency factor, $k$ is Boltzmann constant and $T$ is temperature. The result in Fig. 5.4 is well-fitted by using eq. (5.5), which represent the solid line and $\Delta E$ = 0.43 eV. The quenching of the sample might be assigned to the ionization of Eu 5d level to conduction band of host materials by thermal stimulation. Based on the obtained phonon energy and activation energy above, the configuration coordination model of $Li_2SrSiO_4:Eu^{2+}$ phosphors were proposed as shown in Fig. 5.5. The sum of zero phonon energy $E_0$ and activation energy $\Delta E$ is 2.72 eV which corresponds to the excitation energy from Eu 4f level to the conduction band and probably represents the energy of main PLE band in Fig. 5.1.

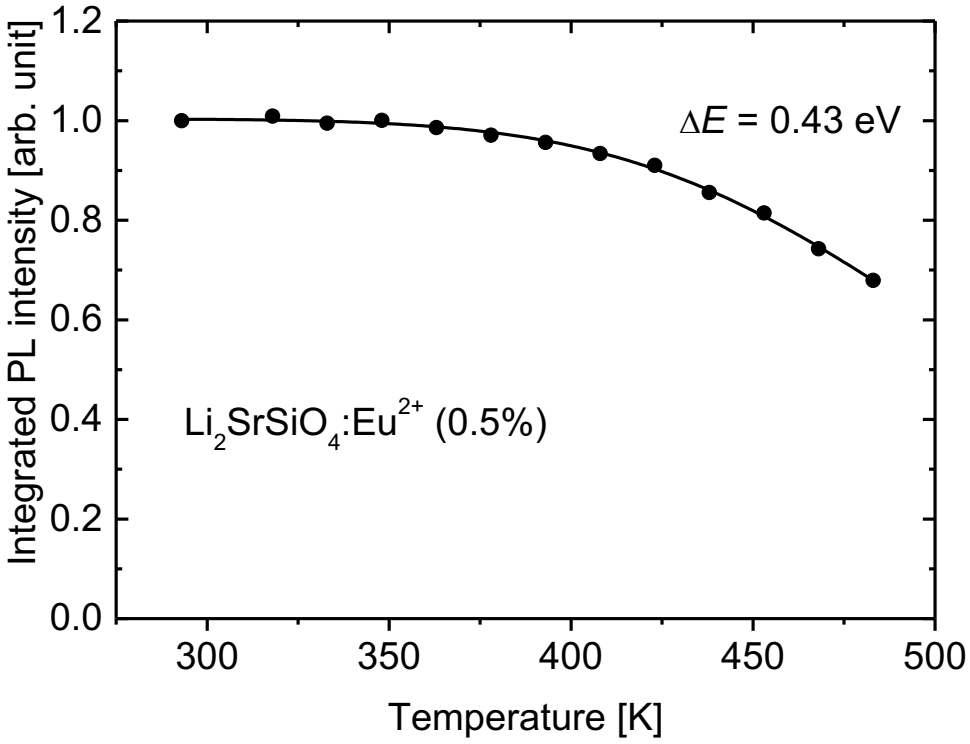


Fig. 5.4 Temperature dependence of integrated PL intensity $Li_2SrSiO_4:Eu^{2+}$ (0.5%) phosphors and fitted by using eq. (5.5)

In this study, the activation energy of $Li_2SrSiO_4:Eu^{2+}$ (0.5%) phosphors show higher activation energy compared to YAG:$Ce^{3+}$ phosphors ($\Delta E$ = 0.14 eV) from previous report [5.3], which reveal that $Li_2SrSiO_4:Eu^{2+}$ phosphors possess high thermal stability. On top of that, quantum efficiency of $Li_2SrSiO_4:Eu^{2+}$ (0.5%) phosphors also was investigated. It was found that quantum efficiency is 62% under 325 nm excitation at room temperature and the CIE 1931 chromaticity coordinates were $x$ = 0.42, $y$ = 0.49, which is in yellow region. Therefore, it is found that $Li_2SrSiO_4:Eu^{2+}$ phosphors have high thermal stability and feasiblity in replacement of YAG:$Ce^{3+}$ phosphors for white LEDs application by combining with blue LED chips.

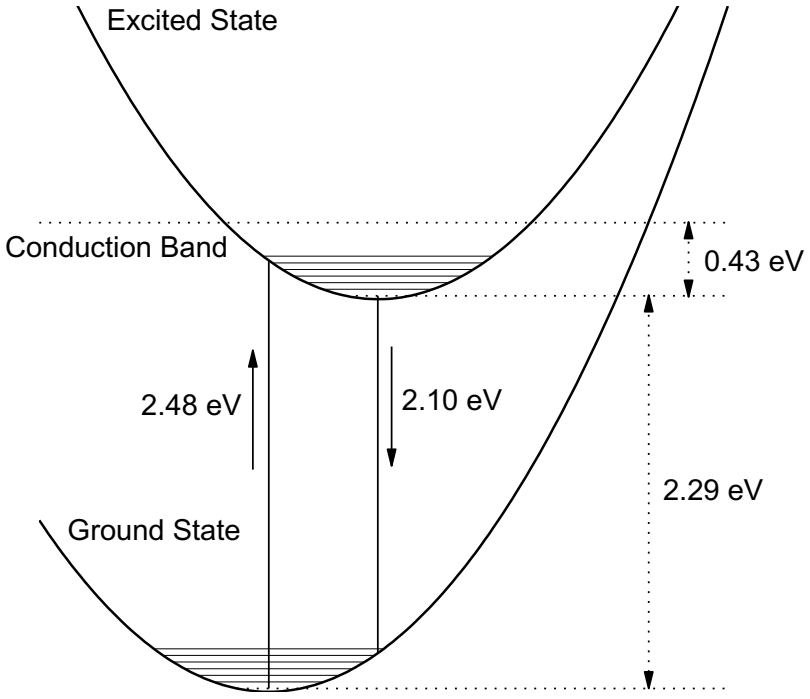


Fig. 5.5 Configuration coordination model of $Li_2SrSiO_4:Eu^{2+}$ phosphors

## 5.4 Conclusion

The thermal stability of $Li_2SrSiO_4:Eu^{2+}$ (0.5%) phosphors were investigated by measuring PL spectra of the samples at both low and high temperature at the temperature range 16 K to 300 K ad 300 K – 483 K respectively. PL spectra of the samples show temperature quenching when increasing in temperature. PL properties in low temperature range were investigated and zero phonon energy and phonon energy associated with emission were found to be 2.29 eV and 38.5 meV respectively based on the fitting with Poisson distribution. Temperature dependence of FWHM of PL band was well reproduced with the phonon energy. From these results, peak energy of PLE and PL bands due to intra Eu transition were estimated to be 2.48 eV and 2.10 eV respectively and the peak energy of PLE band was in blue region, which indicates that $Li_2SrSiO_4:Eu^{2+}$ phosphors can be on of the promising yellow emission with blue excitation phosphor for white LEDs application.

PL intensity at high temprature range from 300 K to 480 K were measured to investigate thermal quenching of the sample. The PL intensity at 423 K was about 80% compared with room temperature, which reveals that $Li_2SrSiO_4:Eu^{2+}$ phosphors have high thermal stability as the temperature in white LEDs reaches 423 K. The temperature depedence of PL intensity due to temperature quenching were well-explained by the Arrhenius equation and it is found that the activation of energy is 0.43 eV. The quenching process might be assigned to the ionization of Eu from 5d excited level to conduction band of host materials by thermal stimulation. The obtained activation energy of $Li_2SrSiO_4:Eu^{2+}$ phosphors show higher activation energy compared to $YAG:Ce^{3+}$ phosphors, 0.14 eV, which also reveal that $Li_2SrSiO_4:Eu^{2+}$ phosphors have high thermal stability.

Moreover, the quantum efficiency of $Li_2SrSiO_4:Eu^{2+}$ phosphors is 62% under 325 nm excitation and the CIE chromaticity coordinates were $x = 0.42$, $y = 0.49$, which is in yellow region. Therefore, it is found that $Li_2SrSiO_4:Eu^{2+}$ phosphors have high thermal stability and

feasiblity in replacement of YAG:$Ce^{3+}$ phosphors for white LEDs application by combining with blue LED chips.

## 5.5 References


[5.1] X. Zhang, M. Gong, A new red-emitting $Ce^{3+}$ , $Mn^{2+}$-doped barium lithium silicate phosphor for NUV LED application, Mater. Lett. 65 (2011) 1756–1758.

[5.2] Z. Wu, J. Liu, M. Gong, Thermally stable luminescence of $SrMg_2(PO_4)_2$:$Eu^{2+}$ phosphor for white light NUV light-emitting diodes, Chem. Phys. Lett. 466 (2008) 88–90.

[5.3] Y. ZHANG, L. LI, X. ZHANG, Q. XI, Temperature effects on photoluminescence of YAG:$Ce^{3+}$ phosphor and performance in white light-emitting diodes, J. Rare Earths. 26 (2008) 446–449.

[5.4] X.Q. Zhang Yanfang. Li Lan, Zhang Xiaosong, Temperature effects on photoluminescence of YAG:$Ce^{3+}$ phosphor and performance in white light-emitting diodes, J. Rare Earths. 26 (2008) 446–449.

[5.5] W. Peng, S. Jun, T. Hua, L.U. Qi-fei, W. Da-jian, Thermal stability of luminous YAG:$Ce^{3+}$ bulk ceramic as a remote phosphor prepared through silica-stabilizing valence of activator in air, Optoelectron. Lett. 8 (2012) 0201–0204.

[5.6] A. Aboulaich, M. Michalska, R. Schneider, A. Potdevin, J. Deschamps, R. Deloncle, G. Chadeyron, R. Mahiou, Ce-doped YAG nanophosphor and red emitting $CuInS_2$/ZnS core/shell quantum dots for warm white light-emitting diode with high color rendering index, ACS Appl. Mater. Interfaces. 6 (2014) 252–258.

[5.7] L. Zhang, J. Zhang, X. Zhang, Z. Hao, G.H. Pan, H. Wu, Site distortion in $Li_2SrSiO_4$: Influence on $Pr^{3+}$ emission and application in wLED, J. Lumin. 180 (2016) 158–162.

[5.8] V.P. Dotsenko, S.M. Levshov, I. V. Berezovskaya, G.B. Stryganyuk, A.S. Voloshinovskii, N.P. Efryushina, Luminescent properties of $Eu^{2+}$ and $Ce^{3+}$ ions in strontium litho-silicate Li2SrSiO4, J. Lumin. 131 (2011) 310–315.

[5.9] X. Zhang, H. He, Z. Li, T. Yu, Z. Zou, Photoluminescence studies on $Eu^{2+}$ and $Ce^{3+}$-doped $Li_2SrSiO_4$, J. Lumin. 128 (2008) 1876–1879.

[5.10] P. You, G. Yin, X. Chen, B. Yue, Z. Huang, X. Liao, Y. Yao, Luminescence properties of $Dy^{3+}$-doped $Li_2SrSiO_4$ for NUV-excited white LEDs, Opt. Mater. 33 (2011) 1808–1812.

[5.11] Z. Wei, Y. Wang, X. Zhu, J. Guan, W. Mao, J. Song, Solid state synthesis and tunable luminescence of $Li_2SrSiO_4:Eu^{2+}/Ce^{3+}$ phosphors, Chem. Phys. Lett. 648 (2016) 8–12.

[5.12] $Li_2SrSiO_4:Eu^{2+}$H. Yu, W.W. Zi, S. Lan, H.F. Zou, S.C. Gan, X.C. Xu, G.Y. Hong, Photoluminescence characteristics of novel red emitting phosphor $Li_2SrSiO_4:Eu^{3+}$, $Sm^{3+}$ for white light emitting diodes, Mater. Res. Innov. 16 (2012) 298–302. https://doi.org/Doi

[5.13] L. Liu, P. You, G. Yin, X. Liao, Z. Huang, X. Chen, Y. Yao, Preparation and photoluminescence properties of the $Eu^{2+}$, $Sm^{3+}$ co-doped $Li_2SrSiO_4$ phosphors, Curr. Appl. Phys. 12 (2012) 1045–1051.

[5.14] H. He, R. Fu, H. Wang, X. Song, Z. Pan, X. Zhao, X. Zhang, Y. Cao, $Li_2SrSiO_4:Eu^{2+}$ phosphor prepared by the Pechini method and its application in white light emitting diode, J. Mater. Res. 12 (2008) 36–39.

[5.15] Y. Li, C. Ni, C.C. Lin, F. Pan, R.S. Liu, J. Wang, Enhancement of UV absorption and near-infrared emission of $Er^{3+}$ in $Li_2SrSiO_4:Ce^{3+}$, $Er^{3+}$ for Ge solar spectral convertor, Opt. Mater. 36 (2014) 1871–1873.

[5.16] M.P. Saradhi, U. V Varadaraju, Photoluminescence Studies on $Eu^{2+}$-Activated $Li_2SrSiO_4$ a Potential Orange-Yellow Phosphor for Solid-State Lighting, Chem. Mater. 18 (2006)

[5.17] H. He, R. Fu, Y. Cao, X. Song, Z. Pan, X. Zhao, Q. Xiao, R. Li, $Ce^{3+} \rightarrow Eu_{2+}$ energy transfer mechanism in the $Li_2SrSiO_4:Eu^{2+}$, $Ce^{3+}$ phosphor, Opt. Mater. 32 (2010) 632–636.

[5.18] S. Cheng, X. Xu, J. Han, J. Qiu, B. Zhang, Design, synthesis and characterization of a novel orange-yellow long-lasting phosphor: $Li_2SrSiO_4:Eu^{2+}$, $Dy^{3+}$, Powder Technol. 276 (2015) 129–133.

[5.19] S.M. Levshov, I. V Berezovskaya, N.P. Efryushina, B.I. Zadneprovskii, V.P. Dotsenko, Synthesis and Luminescence Properties of $Eu^{2+}$-Doped $Li_2SrSiO_4$, Inorg. Mater. 47 (2011) 285–289.

[5.20] L. Chen, A. Luo, Y. Zhang, F. Liu, Y. Jiang, Q. Xu, X. Chen, Q. Hu, S. Chen, K. Chen, H. Kuo, Optimization of the Single-Phased White Phosphor of $Li_2SrSiO_4:Eu^{2+}$, $Ce^{3+}$ for Light-Emitting Diodes by Using the Combinatorial Approach Assisted with the Taguchi Method, Am. Chem. Soc. 14 (2012) 636–644.

[5.21] Y. Rao, X. Hu, T. Liu, X. Zhou, X. Zhou, Y. Li, $Pr^{3+}$-doped $Li_2SrSiO_4$ red phosphor for white LEDs, J. Rare Earths. 29 (2011) 198–201.

[5.22] Y. Hirano, T. Iwata, K. Momma, K. Fukuda, Electron density distribution and crystal structure of lithium strontium silicate, $Li_2SrSiO_4$, Powder Diffr. 25 (2012) 4–8.

[5.23] J. Jeong, K. Jang, H.S. Lee, S.S. Yi, J.H. Jeong, J.H. Park, C. Kim, Photoluminescence Properties of $KSrPO_4:Eu^{2+x}$, $Mn^{2+y}$, and $KSr_{(1-x-y)}PO_4:Eu^{2+x}$, $Mn^{2+y}$ Phosphors for UV-based White LEDs, J. Korean Phys. Soc. 54 (2009) 2390–2395.

[5.24] M.A. Reshchikov, H. Morkǫ, Luminescence properties of defects in GaN, J. Appl. Phys. 97 (2005).

[5.25] S. Bhushan, M. V. Chukichev, Temperature dependent studies of cathodoluminescence of green band of ZnO crystals, J. Mater. Sci. Lett. 7 (1988) 319–321.

# Chapter 6

## Summary and general conclusion

There are abundances of well-known and established research regarding in lighting application and devices, including white LEDs. As we all know, white LEDs have advantages in the aspects of energy consumption, thermal & chemical stability, long lasting, compactness and environmentally sustainable. Nowadays, white LEDs were utilized in everywhere around the world. However, high-power and long-lasting white LEDs required the phosphors with high thermal stability as the deterioration of general white LEDs occurs when the temperature reach at 150 °C during operation. Previous reports predicted that rare earth doped silicate phosphors are promising candidates for white LEDs because of their good photoluminescence properties, thermal stabilities and chemical-physical stabilities. According to Clarke number, silicon is the 2nd most abundance elements exist in earth's crust and silicate compound can easily get to synthesize silicate phosphors. The starting materials in $Sr_2SiO_4:Eu^{2+}$ silicate phosphors are consist of Sr, which are the most suitable elements for the substitution of $Eu^{2+}$ ions, because both Sr and Eu ions have similar ionic radii. Therefore, $Sr_2SiO_4:Eu^{2+}$ silicate phosphors were synthesized as basic phosphors in this study.

Initially, $Sr_2SiO_4:Eu^{2+}$ silicate phosphors were synthesized by improved PCM, where using TEOS as Si source and propylene glycol as chelation agent. Reduction/sintering temperature dependence and Eu concentration dependence of crystal structure and optical properties of $Sr_2SiO_4:Eu^{2+}$ phosphors were investigated. Generally, $Sr_2SiO_4$ have two different crystal phases. (i) α' phase – high temperature phase and (ii) β phase – low temperature phase, with phase transition at 85 °C. Although β phase is stable phase at room temperature, it is quite difficult task to obtain pure β phase $Sr_2SiO_4:Eu^{2+}$ phosphors, because the presence of a few impurities avoid the phase transition during cooling process after synthesis. In this study, β

phase $Sr_2SiO_4:Eu^{2+}$ phosphors were successfully synthesized by improved PCM using HCl sintered at 1150 °C with 3% Eu concentration since intermediate product of $SrCl_2$ act as flux to remove impurities. Phase transition of the β phase $Sr_2SiO_4:Eu^{2+}$ phosphors were also investigated by measuring PL spectra and XRD of the samples under the heating and cooling cycles of 30 °C – 110 °C – 30 °C and 30 °C – 200 °C – 30 °C, respectively. As the temperature increases, the samples are getting into the α' phase. Meanwhile, the samples are getting into β phase as temperature decreases. α' → β phase transition can be observed at 100 °C and 80 °C at XRD and PL results, respectively. β → α' phase transition can be observed around 70 °C and 60 °C at XRD and PL results, respectively. These results indicate that the hysteresis of the samples can be observed. The further analysis show that the thermal hysteresis between β ↔ α' directions of $Sr_2SiO_4:Eu^{2+}$ phosphors are about 40 K, which is much larger than the reported thermal hysteresis of undoped $Sr_2SiO_4$ from the previous report, suggesting that the addition or doping of Eu impurities prevent the phase transition. This study indicates that good properties of $Sr_2SiO_4:Eu^{2+}$ phosphors can be synthesized by improved PCM. However, this Eu doped silicate phosphors show phase green emission, which does not meet the research objective to use the combination of yellow phosphors and blue LEDs in producing white LEDs. As $Sr_2SiO_4:Eu^{2+}$ phosphors have phase transition, which is not suitable for white LED application, Li introduction were suggested in this study to fix the phase transition in the host lattice and tune emission wavelength to be suitable for white LEDs.

$Li_2SrSiO_4:Eu^{2+}$ silicate phosphor is one of the promising luminescent materials, which possess blue excitation yellow phosphor with advantages in the aspect of chemical-physical stability, high luminous intensity and expected to be high thermal stability. From the investigation on sintering/reduction temperature dependence and Eu concentration dependence, the optimum synthesis of $Li_2SrSiO_4:Eu^{2+}$ phosphors are 900 °C sintering/reduction temperature and 0.5% Eu concentration. After obtaining the optimum synthesis of $Li_2SrSiO_4:Eu^{2+}$

phosphors, the thermal stability of the samples were investigated. From the PL results, Eu concentration quenching and temperature quenching of the samples can be observed. The PL intensity at 150 °C ( 423 K ) was about 80% compared with room temperature, which reveals that $Li_2SrSiO_4:Eu^{2+}$ phosphors have high thermal stability. It is found that the activation of energy is 0.43 eV. The quenching process might be assigned to the ionization of Eu from 5d excited level to conduction band of host materials by thermal stimulation. The obtained activation energy of $Li_2SrSiO_4:Eu^{2+}$ phosphors show higher activation energy compared to generally commercialized $YAG:Ce^{3+}$ phosphors, 0.14 eV, which also reveal that $Li_2SrSiO_4:Eu^{2+}$ phosphors have high thermal stability. In addition, the quantum efficiency of $Li_2SrSiO_4:Eu^{2+}$ phosphors is 62% under 325 nm excitation and the CIE chromaticity coordinates were $x$ = 0.42, $y$ = 0.49, which is in yellow region. Therefore, it is found that $Li_2SrSiO_4:Eu^{2+}$ phosphors have high thermal stability and feasiblity in replacement of $YAG:Ce^{3+}$ phosphors for white LEDs application. The study also shows that improved PCM was successfully demonstrated in both silicate phosphors.

From above researches, both silicate phosphors; $Sr_2SiO_4:Eu^{2+}$ and $Li_2SrSiO_4:Eu^{2+}$ phosphors were successfully synthesized by improved PCM using TEOS, which has advantaged in the aspect of uniformity of atomic component of the samples and low synthetization temperature. Initially synthesized $Sr_2SiO_4:Eu^{2+}$ green phosphors show phase transition and the hysteresis can be observed owing to improved PCM. After that, $Li_2SrSiO_4:Eu^{2+}$ yellow phosphors were synthesized by improved PCM to fix the phase trasition and tune emission wavelength of $Sr_2SiO_4:Eu^{2+}$ phosphors by Li introduction. The results show that synthesized $Li_2SrSiO_4:Eu^{2+}$ phosphors show high thermal stability, which feasible replacement of commercialized $YAG:Ce^{3+}$ yellow phosphors in white LEDs. Therefore, this study demonstrated that usability of improved PCM for silicate phosphor research and the utilization of $Li_2SrSiO_4:Eu^{2+}$ in white LEDs application.

# Publications

- Luminescence properties of $Li_2SrSiO_4:Eu^{2+}$ silicate yellow phosphors with high thermal stability for high-power efficiency white LED application,
  Siti Sarina Binti Nasir, Akihiro Tanaka, Shuto Yoshiara, Ariyuki Kato,
  Journal of Luminescence, 207 (2018) 22-28.
- Effect of Eu doping on room temperature phase and phase transition $Sr_2SiO_4:Eu^{2+}$ phosphor synthesized by polymerized complex method,
  Siti Sarina Binti Nasir, Kouta Yakura, Noriyuki Horiuchi, Masaya Tsuta, Ariyuki Kato,
  Journal of Physics and Chemistry of Solids, 133 (2019) 135 – 141.

# Conferences

**International conferences**

- Phase Control of Eu-doped $Sr_2SiO_4$ Phosphor by Eu Concentration and Sintering Temperature,
  Siti Sarina Binti Nasir, Kouta Yakura, Noriyuki Horiuchi, Ariyuki Kato,
  6th International Symposium on Organic and Inorganic Electronic Materials and Related Nanotechnologies (EM-NANO 2017), PO2-32 (June 18-21, 2017, Fukui Prefectural Hall, Japan).
- Synthesis of $Li_2SrSiO_4:Eu^{2+}$ Nano Phosphor by Reverse Micelle,
  Siti Sarina Nasir, Kato Ariyuki,
  5th International GIGAKU Conference in Nagaoka (IGCN 2016), P-22, (October 6-7, 2016, Nagaoka University of Technology, Japan).
- Synthesis of $SrCu_2O_2:Eu^{2+}$ Phosphor by Solid State Reaction Method,
  Siti Sarina Binti Nasir, Ariyuki Kato,
  3rd International GIGAKU Conference in Nagaoka (IGCN 2014), MP-18, (June 20-22, 2014, Nagaoka University of Technology, Japan).

- Synthesis of the $Li_2SrSiO_4:Eu^{2+}$ Yellow Phosphor by Polymerized Complex Method, Siti Sarina Binti Nasir, Akihiro Tanaka and Ariyuki Kato,
  JSAP-MRS Joint Symposia, 18p-PM2-24, (September 16-20, 2013, Doshisha University, Japan).

**Domenstic conference**

- 逆ミセル法による Eu 添加ストロンチウムケイ酸塩ナノ蛍光体の作製,
  シティ・サリナ・ビンティ・ナシル，松原寿樹，加藤有行,
  第 64 回応用物理学会春季学術講演会，16p-P7-13（2017 年 3 月 14〜17 日，パシフィコ横浜.

# Acknowledgement

In the name of Allah, the Most Gracious and the Most Merciful

First of foremost, all praise to Allah and His blessing for the completion of this dissertation. I would like to acknowledge and express my utmost gratitude to Allah S.W.T for His guidance and blessing that bestowed upon me by giving me opportunity, courage, trials and strength to complete this research and finally able to complete the dissertation, which was physically and mentally challenging.

Undertaking this study journey (Undergraduate, Master and PhD) in Nagaoka University Japan has been a truly life-changing experience for me and it would not have been possible to do without the support and guidance that I received from so many people. I would like to express my deepest gratitude and appreciation to my supervisor, Associate Professor Ariyuki Kato for his excellent guidance, tremendous support, unwavering patience, insightful reminders and much needed motivation towards the inception of the research journey until its achievement of its objective and dissertation submission. As I am the only Malaysian student, girl, Muslim and the first PhD student in the lab, it is quite challenging for me to adapt with the surrounding with other Japanese students. However, my supervisor always concern and understanding so that I can perform well as other Japanese students.

I would also like to extend my deepest gratitude to Professor Munehiro Kimura, Professor Kunihiko Tanaka, Associate Professor Tomoichiro Okamoto and Associate Professor Takeya Unuma as examiner during preliminary examination for their guidance, valuable advices and ingenious suggestion to improve this dissertation and get me prepare for the final presentation. On top of that, I am indebted to The Uchida Energy Science Promotion Foundation （内田エネルギー科学振興財団）for providing the grant and resources throughout my research period. Besides that, I am also grateful to have supportive laboratory members who always helping me in my lab works, Japanese lessons and others.

My study in Japan would not have been possible without the scholarship from Yayasan Pelajaran MARA (YPM) from 2011 until 2018, which removed financial concerns from my decision to embark on this journey. I am extremely grateful for the scholarship as well as opportunity to further my study in Japan from Undergraduate, Master until PhD wherein I can educate, enrich and enlighten many things through my bitter and sweet experiences here. I hope that this dissertation is worth for bringing up the pride as Malaysian student in Japan.

Being away from home for 8 years, the moral and emotional support from Malaysian community in Nagaoka, Japan played a vital role in encourage and uplifting me for accomplishing this research and dissertation. Although being far away from home, they continuously serve as proponent source of unconditional and make my heart feels like home. Special thanks to my juniors especially Sofia Imana and Amalina Aina for always being helping hands and understanding. I will never forget their kindness and may God shower them with success and honour in their life.

I will never forget to extend my deepest gratitude to my family (papa, mama, and siblings) who are very important existence in my life. The most unforgettable incident happened when my late papa who always giving continuously courage and valuable advices to me, suddenly passed away during my second year in PhD journey. It totally effect physically and emotionally to my whole family especially to myself. Although my family was still grieving at that time, they never told me to stop my PhD journey as this was my papa's dream to see me holding PhD scroll. Continuous support and prayers from my family are the reasons for me to never give up in this PhD journey.

Lastly, special thanks to lovely husband for very helpful, understanding and continuous support especially during my critical time to finish up everything for my dissertation and preparation for my final presentation in my PhD journey. Besides that, I am very grateful and feel blessed to have lovely son in my life. Many thanks to my son for his understanding and bear with me along my PhD journey. I also truly want to apologize if he feels lonely and unattended while I am busy doing my dissertation and final presentation. No matter what, I love my little family.

Sincerely,
SITI SARINA BINTI NASIR